nature cell biology

Deciphering the transcriptional complex critical for *RhoA* gene expression and cancer metastasis

Chia-Hsin Chan[1], Szu-Wei Lee[1,2,11], Chien-Feng Li[3,11], Jing Wang[1,6], Wei-Lei Yang[1,2], Ching-Yuan Wu[1,4,5], Juan Wu[1,6], Keiichi I. Nakayama[7], Hong-Yo Kang[5], Hsuan-Ying Huang[8], Mien-Chie Hung[1,2,9], Pier Paolo Pandolfi[10] and Hui-Kuan Lin[1,2,12]

The RhoA GTPase is crucial in numerous biological functions and is linked to cancer metastasis. However, the understanding of the molecular mechanism responsible for *RhoA* transcription is still very limited. Here we show that *RhoA* transcription is orchestrated by the Myc–Skp2–Miz1–p300 transcriptional complex. Skp2 cooperates with Myc to induce *RhoA* transcription by recruiting Miz1 and p300 to the *RhoA* promoter independently of Skp1-Cullin-F-box protein containing complex (SCF)–Skp2 E3 ligase activity. Deficiency of this complex results in impairment in RhoA expression, cell migration, invasion, and breast cancer metastasis, recapitulating the phenotypes observed in RhoA knockdown, and RhoA restoration rescues the defect in cell invasion. Overexpression of the Myc–Skp2–Miz1 complex is found in metastatic human cancers and is correlated with RhoA expression. Our study provides insight into how oncogenic Skp2 and Myc coordinate to induce *RhoA* transcription and establishes a novel SCF–Skp2 E3-ligase-independent function for oncogenic Skp2 in transcription and cancer metastasis.

Cancer metastasis is a complex process involving several key steps that allow disseminating primary cancer cells to colonize distant sites[1,2]. It causes most of the deaths of patients with cancer, and the treatment of this devastating form of disease remains a big challenge.

RhoA, a well-known member of the Rho family of GTPases, regulates numerous biological functions and is implicated in cancer metastasis[3,4]. Although mutation of RhoA has not been found in human cancers[4–6], upregulation of *RhoA* mRNA and RhoA protein levels have been well documented in various human cancers[7–9]. Moreover, RhoA overexpression overcomes senescence checkpoints and induces preneoplastic transformation of human mammary epithelial cells[10], whereas RhoA deficiency suppresses the invasiveness of breast cancer cells[11]. A recent study also demonstrated that microRNA-31 (miR-31) suppresses breast cancer metastasis partly through downregulation of *RhoA* gene expression[12]. Although accumulating evidence unequivocally shows that RhoA overexpression is positively correlated with cancer metastasis[13,14], the transcription machinery responsible for *RhoA* gene expression has so far been unknown.

The Myc transcription factor heterodimerizes with Max and binds to the E-box motif CACGTG to activate transcription by cooperating with multiple coactivator complexes[15–17]. It serves a master regulator in various biological functions and is linked to metastasis. Recent studies demonstrate that Myc ubiquitylation is critical in Myc transcriptional activation in a subset of target genes that are important for cell proliferation[18–20]. Although a handful of Myc target genes involved in Myc-driven cell-cycle progression and apoptosis have been identified, its target genes responsible for Myc-mediated cell migration and metastasis still remain elusive.

In this study we sought to identify the transcription machinery critical for *RhoA* transcription and cancer metastasis. Our study reveals that the Myc–Skp2–Miz1 transcriptional complex is critical for *RhoA* gene transcription, cell invasion and cancer metastasis.

RESULTS

Myc serves a transcription factor for RhoA

To explore the transcriptional machinery for *RhoA*, we analysed the 5′ sequence upstream of the transcription start site up to 9 kilobase pairs (kb)

[1]Department of Molecular and Cellular Oncology, The University of Texas M. D. Anderson Cancer Center, Houston, Texas 77030, USA. [2]The University of Texas Graduate School of Biomedical Sciences at Houston, Houston, Texas 77030, USA. [3]Department of Pathology, Chi-Mei Medical Center, Tainan 710, Taiwan. [4]Department of Chinese Medicine, Chang Gung Memorial Hospital Medical Center, Chang Gung University, College of Medicine, Kaohsiung 833, Taiwan. [5]Graduate Institute of Clinical Medical Sciences, Chang Gung Memorial Hospital Medical Center, Chang Gung University, College of Medicine, Kaohsiung 833, Taiwan. [6]State Key Laboratory of Oncology in South China and Department of Experimental Research, Sun Yat-Sen University Cancer Center, Guangzhou, 510060, China. [7]Department of Molecular and Cellular Biology, Medical Institute of Bioregulation, Kyushu University, Fukuoka 812-8582, Japan. [8]Department of Pathology, Chang Gung Memorial Hospital–Kaohsiung Medical Center, Chang Gung University College of Medicine, Kaohsiung 833, Taiwan. [9]Center for Molecular Medicine and Graduate Institute of Cancer Biology, China Medical University and Hospital, Taichung 404, Taiwan. [10]Cancer Genetics Program, Beth Israel Deaconess Cancer Center and Department of Medicine and Pathology, Beth Israel Deaconess Medical Center, Harvard Medical School, Boston, Massachusetts 02215, USA.
[11]These authors contributed equally to this work.
[12]Correspondence should be addressed to Hui-Kuan Lin: hklin@mdanderson.org

Received 4 January 2010; accepted 1 March 2010; published online 11 April 2010; DOI:10.1038/ncb2047

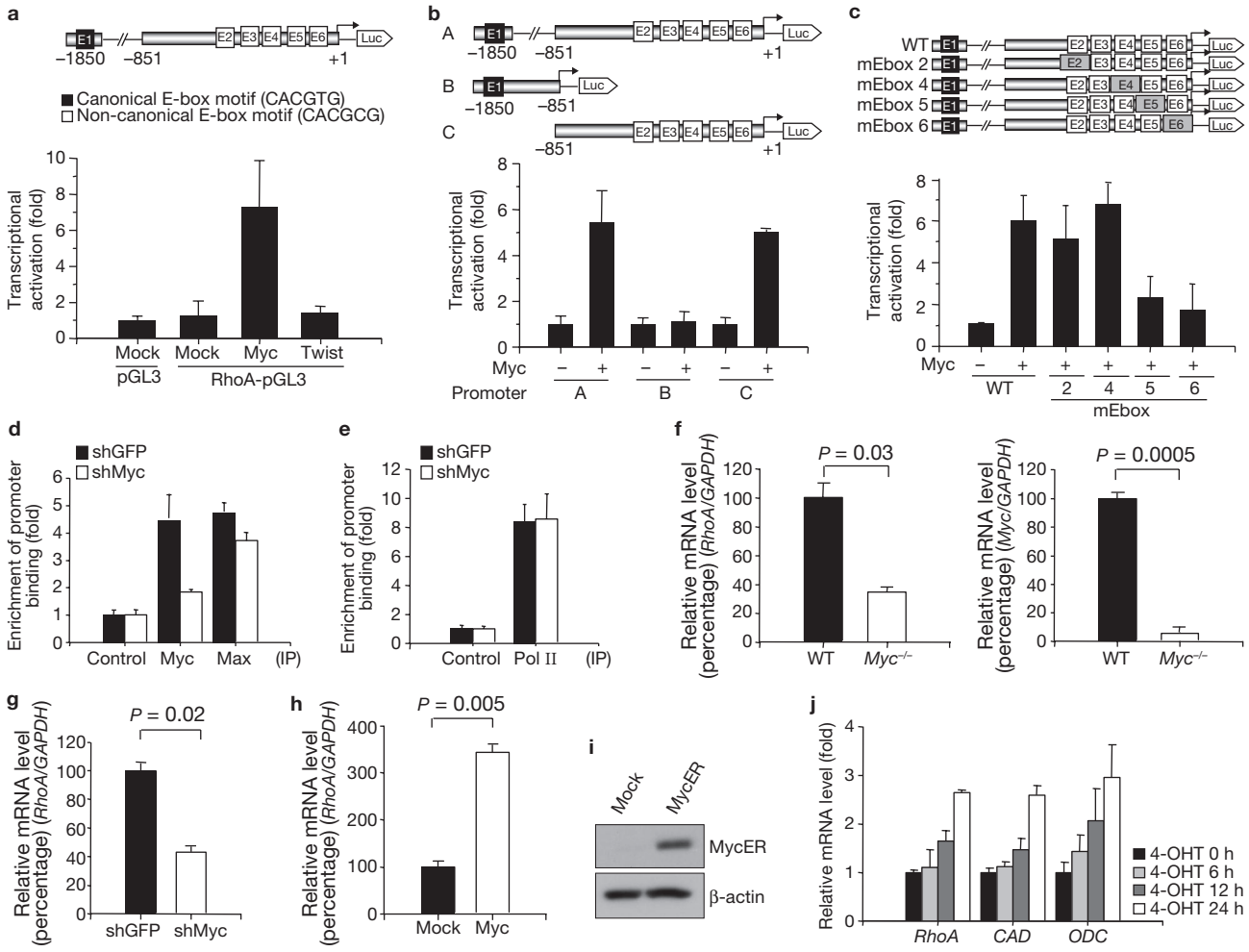

Figure 1 Myc is a transcription factor for RhoA. (**a**) 293T cells were transfected with the indicated plasmids and harvested for a RhoA reporter assay. (**b**) *RhoA* promoter fragment constructs used for the reporter assay. (**c**) Reporter assay in 293T cells transfected with various *RhoA* promoter constructs with mutations in different E-box regions (mEbox). WT, wild-type. (**d**, **e**) ChIP assay for *RhoA* promoter (**d**) or *GAPDH* promoter (**e** in PC-3 cells with GFP or Myc knockdown. Myc knockdown efficiency is shown in the left panel of Fig. 2b. Pol II, RNA polymerase II. (**f**) Analysis of RhoA and Myc mRNA levels in WT and *Myc*-null Rat1 cells by real-time PCR. The quantified results are presented as means ± s.d. ($n = 3$). (**g**) Analysis of *RhoA* mRNA levels in MDA-MB-231 cell lines infected with GFP or Myc knockdown. (**h**) Analysis of *RhoA* mRNA levels in MDA-MB-231 cell lines infected with murine stem cell virus (MSCV) or MSCV-Myc. (**i**) Western blot analysis of Myc protein expression in MDA-MB-231 cells infected with pBabe or pBabe-MycER. (**j**) Analysis of *RhoA*, *CAD* and *ODC* mRNA levels in MDA-MB-231 cell lines following the time course of MycER activation induced by 4-OHT. Results in **a**–**c** are shown as means ± s.d. of one representative experiment (**a**, **c** from four independent experiments; **b** from three independent experiments) performed in triplicate. Results in **d**–**h** and **j** are presented as means ± s.d. ($n = 3$). Uncropped images of blots are shown in Supplementary Information, Fig. S11.

with the computer program TFSEARCH (http://www.cbrc.jp/research/db/TFSEARCH.html). We found that there is one canonical (CACGTG) and five non-canonical (CACGCG) E-boxes present within 2 kb upstream of transcription start site (Fig. 1a), reminiscent of the binding sites for Myc and Twist[17,21,22]. Myc and Twist contribute to multiple steps of tumorigenesis and are linked to cancer metastasis[16,21–24]. To determine the role of Myc and Twist in *RhoA* transcription, we cloned this human *RhoA* promoter fragment (nucleotides −1850 to +1) into the pGL3 luciferase vector for a luciferase activity assay. *RhoA* transcriptional activity and protein expression were induced by Myc overexpression but not by Twist overexpression (Fig. 1a; Supplementary Information, Fig. S1a, b). This result suggests that *RhoA* transcription is selectively induced by Myc.

To dissect the promoter region required for *RhoA* transcription by Myc, we generated two fragments from the full-length *RhoA* promoter. To our surprise, the transcriptional activity of the distal region (fragment B) containing the canonical E-box motif was not induced by Myc, whereas the transcriptional activity of fragment C containing five non-canonical E-box motifs was readily induced by Myc (Fig. 1b), suggesting that Myc may affect *RhoA* transcription by recognizing any one of five non-canonical E-box motifs within fragment C. To validate this notion, we mutated these non-canonical E-box motifs individually and used them in a reporter assay. We successfully generated full-length *RhoA* promoters with mutations in E-box 2, 4, 5 or 6 located within fragment C; a promoter with mutations in E-box 3 was not obtained because of its GC-rich content. The basal transcriptional activity of these promoters was not affected by the mutations (Supplementary Information, Fig. S1c). Although mutations in E-boxes 2 and 4 did not significantly affect the ability

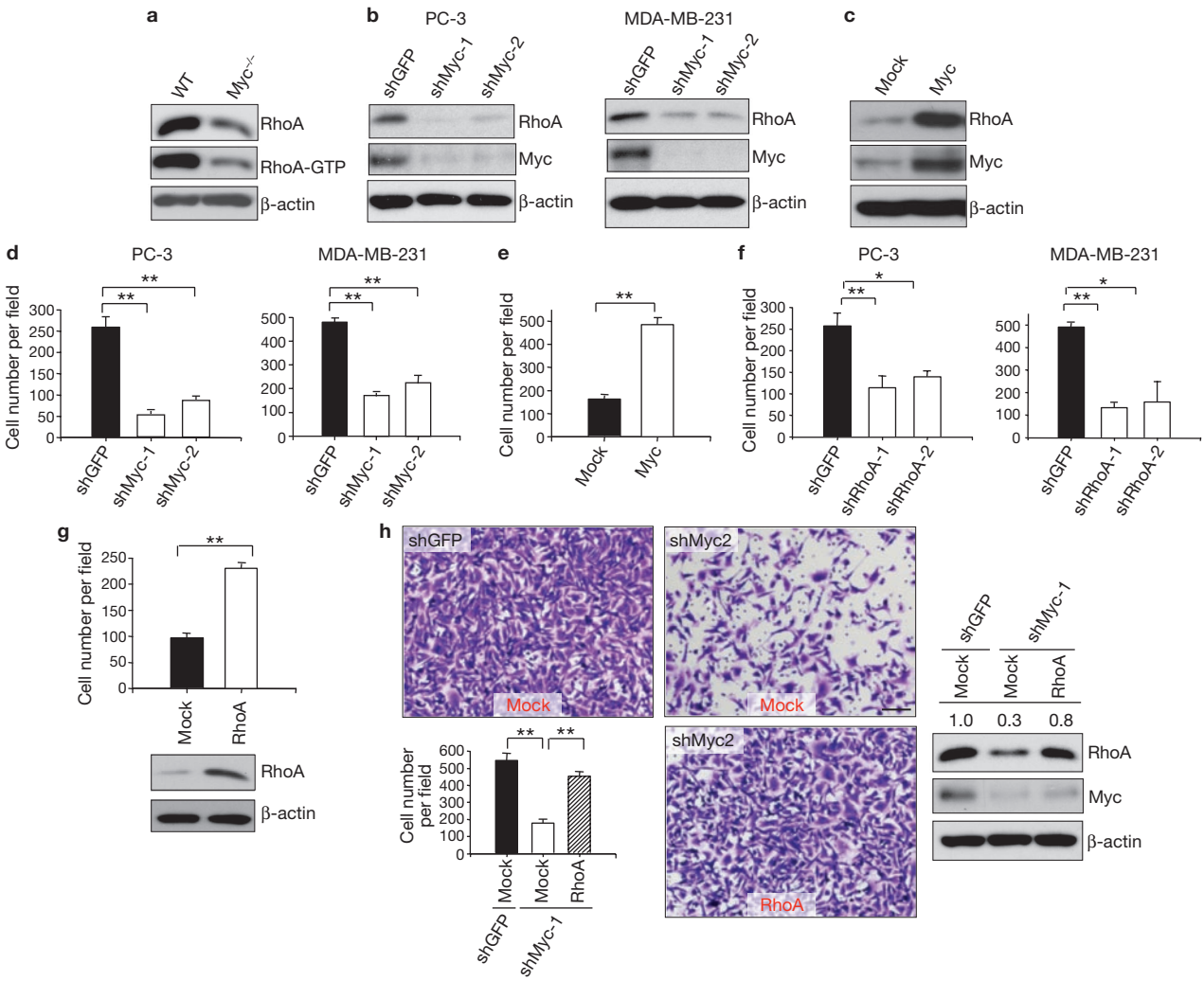

Figure 2 Myc regulates cell invasion through RhoA. (**a**) Western blot analysis of active RhoA (RhoA–GTP) and total RhoA expression in WT Myc and *Myc*-null Rat1 cells. (**b**) Western blot analysis of RhoA expression in two cancer lines with GFP or Myc knockdown. Two Myc lentiviral short hairpin RNAs (shRNAs) were used in this assay. (**c**) Western blot analysis of RhoA expression in MDA-MB-231 cells infected with MSCV or MSCV-Myc. (**d**) Matrigel cell invasion assay in two cancer cell lines with GFP or Myc knockdown. (**e**) Matrigel cell invasion assay in MDA-MB-231 cells infected with MSCV or MSCV-Myc. (**f**) Matrigel cell invasion assay in two cancer cell lines with GFP or RhoA knockdown. Two RhoA lentiviral shRNAs were used in this assay. (**g**) Matrigel cell invasion assay and western blot analysis in MDA-MB-231 cells infected with MSCV or MSCV-RhoA. (**h**) Matrigel cell invasion assay and western blot analysis in MDA-MB-231 cells with GFP, Myc knockdown or with Myc knockdown plus RhoA overexpression. The relative intensity of RhoA was quantified with ImageQuant software and normalized with β-actin. The quantified results are presented as means ± s.d. ($n = 4$). Asterisk, $P < 0.05$; two asterisks, $P < 0.01$. Scale bar, 100 μm. Uncropped images of blots are shown in Supplementary Information, Fig. S11.

of Myc to induce *RhoA* transcription activation, mutations in either E-box 5 or E-box 6 impaired the effect of Myc on *RhoA* transcription activation (Fig. 1c), suggesting that Myc may bind to E-box 5 and 6 to regulate *RhoA* transcription.

To corroborate this notion, we performed *in vivo* chromatin immunoprecipitation (ChIP) assays to address whether Myc binds to the *RhoA* promoter region surrounding E-boxes 5 and 6. The ChIP assay revealed that endogenous Myc binds to E-boxes 5 and 6, whereas Myc knockdown attenuated this effect (Figs 1d and 2b). We found that Max was also present in this *RhoA* promoter, but the recruitment of Max to this *RhoA* promoter was only slightly affected by Myc knockdown (Fig. 1d). Control experiments showed that RNA polymerase II bound to the *glyceraldehyde-3-phosphate dehydrogenase* (*GAPDH*) promoter irrespective of Myc expression (Fig. 1e). Real-time PCR revealed that *RhoA* mRNA in *Myc*-null cells was much lower than in wild-type cells (Fig. 1f). Similarly, Myc knockdown decreased *RhoA* mRNA expression, whereas Myc overexpression induced it (Fig. 1g, h).

We examined the kinetics of *RhoA* transcription by using an inducible MycER system[20,25]. MDA-MB-231 cells with stable MycER expression were generated, treated with 4-hydroxytamoxifen (4-OHT) to activate MycER proteins, and harvested for RhoA expression (Fig. 1i). *RhoA* mRNA levels were induced after MycER activation by 4-OHT in a time-dependent manner, similar to those encoding carbamoyl-phosphate synthetase 2, aspartate transcarbamylase and dihydroorotase (CAD) and ornithine decarboxylase (ODC), two known Myc target genes[26,27] (Fig. 1j). These results suggest that Myc serves as a transcriptional factor to activate *RhoA* transcription.

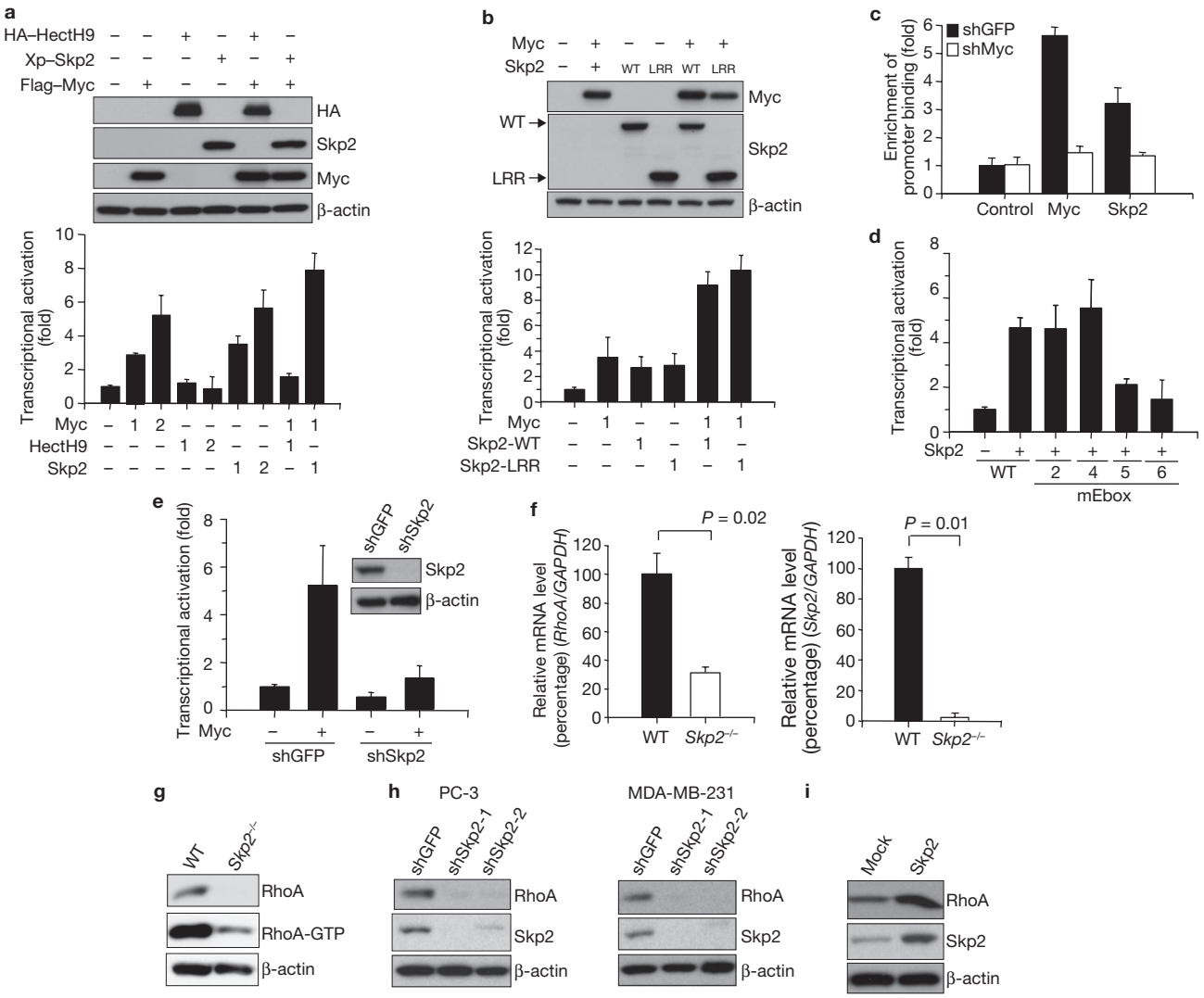

Figure 3 Skp2 cooperates with Myc to regulate *RhoA* transcription independently of Myc ubiquitylation and SCF–Skp2 E3 ligase activity. (**a**, **b**) RhoA reporter assay in 293T cells transfected with Myc, HectH9 and Skp2 plasmids (**a**), or Myc, Skp2-WT and Skp2-LRR plasmids (**b**). In the lower panel, the numbers indicate the amount (μg) of each plasmid used in this assay. HA, haemagglutinin. Upper panel: western blot analysis showing the expression of constructs as indicated. (**c**) ChIP assay in PC-3 cells with GFP or Myc knockdown. The quantified results are presented as means ± s.d. ($n = 3$). (**d**) RhoA reporter assay in 293T cells transfected with various *RhoA* promoter constructs with mutations in different E-box regions. (**e**) RhoA reporter assay in 293T cells with GFP or Skp2 knockdown. Inset: western blot analysis of Skp2 expression in 293T cells with GFP or Skp2 knockdown. (**f**) Analysis of RhoA and Skp2 mRNA levels in WT and *Skp2*$^{-/-}$ primary MEFs by real-time PCR. The quantified results are presented as means ± s.d. ($n = 3$). (**g**) Western blot analysis of active RhoA (RhoA-GTP) and total RhoA expression in WT and *Skp2*$^{-/-}$ primary MEFs. (**h**) Western blot analysis of RhoA expression in various cancer cell lines infected with GFP shRNA or Skp2 shRNA. Two Skp2 lentiviral shRNAs were used in this assay. (**i**) Western blot analysis in PC-3 cells infected with pBabe or pBabe-Skp2. Results in **a**, **b**, **d** and **e** are shown as means ± s.d. of one representative experiment (from three independent experiments) performed in triplicate. Uncropped images of blots are shown in Supplementary Information, Fig. S11.

RhoA mediates Myc-regulated cell migration and invasion

We next determined whether Myc levels are critical for RhoA protein expression and activity. Both RhoA protein expression and RhoA activity were greatly decreased in *Myc*-null cells, indicating that Myc regulates RhoA protein expression and in turn affects RhoA activity (Fig. 2a). Similarly, knockdown of Myc expression profoundly decreased RhoA protein expression in cancer cells, whereas Myc overexpression promoted it (Fig. 2b, c). RhoA protein expression was also induced after the MycER activation, in a time-dependent manner (Supplementary Information, Fig. S1d). Because RhoA is critical in cell migration and invasion[3,4], we determined the function of Myc in these processes. Myc knockdown in cancer cells robustly attenuated cell migration and invasion, whereas Myc overexpression promoted these processes (Fig. 2d, e; Supplementary Information, Fig. S1e, h). RhoA knockdown or overexpression phenocopied the effects of Myc on cell migration and invasion (Fig. 2f, g; Supplementary Information, Fig. S1f, g, i), raising the possibility that Myc may regulate these processes by affecting RhoA expression. In support of this notion we found that restoration of RhoA expression rescued a cell invasion defect in Myc-knockdown cells (Fig. 2h). The effect of Myc and RhoA deficiency on cell migration and invasion was not due to their ability to regulate cell proliferation and apoptosis, because Myc and RhoA knockdown did not significantly affect either cell proliferation or apoptosis within 2 days, given that all our migration and invasion assays were performed within 24 h (Supplementary Information, Fig. S2a–c). However, Myc

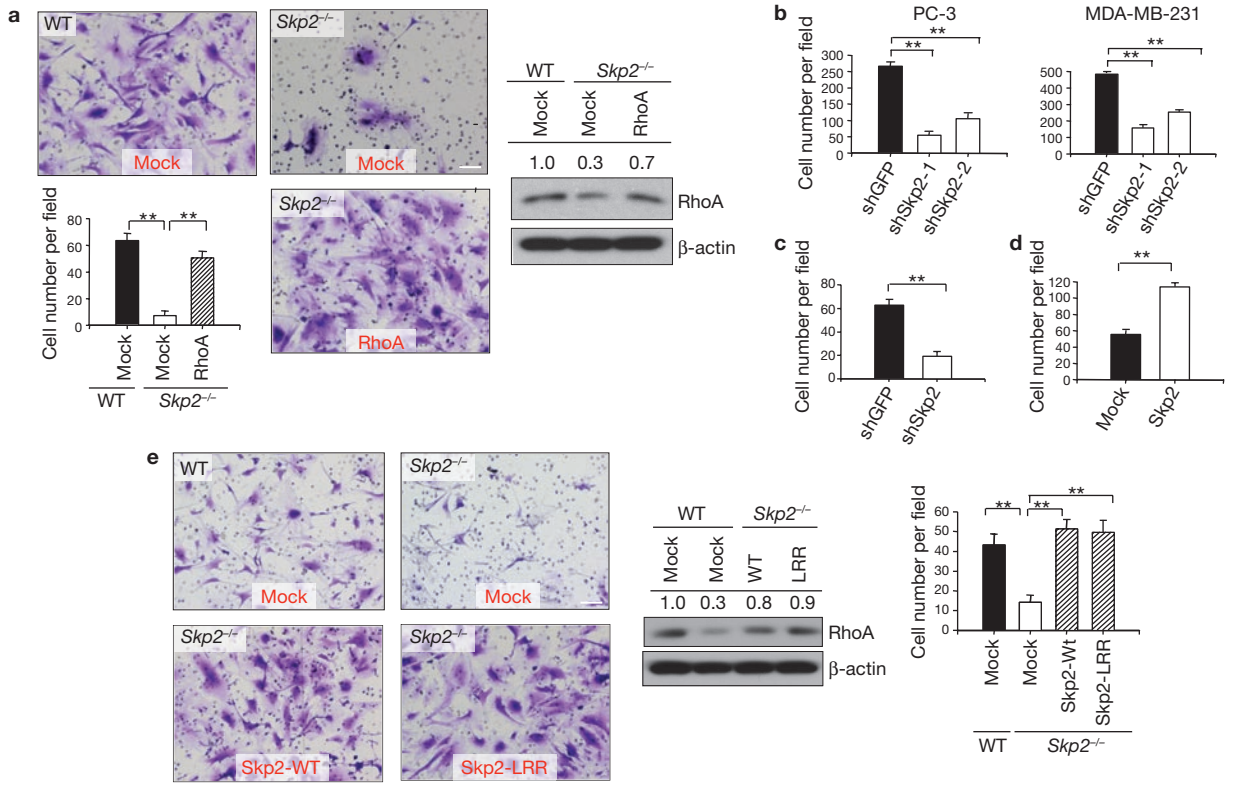

Figure 4 Skp2 regulates cell invasion independently of SCF–Skp2 E3 ligase activity. (**a**) Matrigel cell invasion assay and western blot analysis of RhoA expression in WT and *Skp2*$^{-/-}$ primary MEFs infected with MSCV or MSCV-RhoA. (**b**) Matrigel cell invasion assay in two cancer cell lines infected with GFP or Skp2 knockdown. (**c**) Transwell cell migration assay in PC-3 cells infected with GFP or Skp2 knockdown. (**d**) Transwell cell migration assay in PC-3 cells infected with pBabe or pBabe-Skp2. (**e**) Matrigel cell invasion assay and western blot analysis of RhoA expression in WT and *Skp2*$^{-/-}$ primary MEFs infected with pBabe, pBabe-Skp2 or pBabe-Skp2-LRR as indicated. The relative intensities of RhoA were quantified with ImageQuant software and normalized with β-actin. Results in **b**–**e** are shown as means ± s.d. ($n = 4$). Asterisk, $P < 0.05$; two asterisks, $P < 0.01$. Scale bar, 100 μm. Uncropped images of blots are shown in Supplementary Information, Fig. S11.

knockdown significantly inhibited cell proliferation at later time points and also primary tumour formation (Supplementary Information, Fig. S2a, d), supporting its oncogenic functions[16,17]. Our results identify RhoA as a critical effector for Myc-mediated cell migration and invasion.

Skp2 cooperates with Myc to promote *RhoA* transcription independently of SCF–Skp2 E3 ligase activity

Although ubiquitylation is thought to regulate protein degradation, recent studies suggest that ubiquitylation also has a non-proteolytic role in the control of transcription[28,29]. HectH9 and Skp2 E3 ligases have been shown to induce Myc ubiquitylation and to cooperate with Myc to induce a subset of target genes important for cell-cycle progression and proliferation[18–20]. To investigate whether Myc ubiquitylation is also important for Myc-mediated *RhoA* transcription, we examined the effect of HectH9 and Skp2 on *RhoA* transcription. HectH9 overexpression failed to promote *RhoA* transcriptional activation, protein expression and Myc-mediated *RhoA* transcription, although it induced Myc ubiquitylation (Fig. 3a; Supplementary Information, Fig. S3a, b)[18]. Moreover, we found that HectH9 was not required for RhoA protein expression and the ability of Myc to induce *RhoA* transcription (Supplementary Information, Fig. S3c, d). These results suggest that a subset of Myc target genes such as RhoA are not regulated by HectH9 and HectH9-mediated Myc ubiquitylation. However, we found that *RhoA* transcription was induced by Skp2 overexpression, and a synergistic effect on *RhoA* transcription was observed on overexpression of Skp2 and Myc (Fig. 3a). Skp2 is an F-box protein that forms a Skp2–SCF complex with Skp1, Cullin-1 and Rbx1 to constitute an E3 ligase activity, and its F-box domain is required for SCF–Skp2 E3 ligase activity and Skp2 oncogenic functions[30,31]. Because Skp2 regulated Myc ubiquitylation (Supplementary Information, Fig. S3e), we wished to determine whether SCF–Skp2 E3 ligase activity is required for the effect of Skp2 on *RhoA* transcription. Consistent with the previous reports[19,32] was our finding that the Skp2-LRR mutant devoid of the amino terminus and F-box domain failed to form a Skp2–SCF complex and lost its E3 ligase activity towards promoting the ubiquitylation of p27 and Myc (Supplementary Information, Fig. S4a–c), two well-known Skp2 substrates[19,20,30,31]. Skp2-LRR synergized with Myc to activate *RhoA* transcription in the same way as wild-type Skp2 did (Fig. 3b). This result suggests that SCF–Skp2 E3 ligase activity and Myc ubiquitylation induced by Skp2 are not critical for *RhoA* transcription.

We next determined whether Skp2-induced *RhoA* transcription requires Myc. The ChIP assay demonstrated that both endogenous Skp2 and Myc bind to the *RhoA* promoter, and Myc knockdown prevented Skp2 from binding to this promoter (Fig. 3c), suggesting that Myc recruits Skp2 to the *RhoA* promoter to activate *RhoA* transcription. This notion was further supported by the fact that Skp2 failed to activate *RhoA* promoters with mutations in either E-box 5 or E-box 6, the region critical for Myc binding (Figs 1c and 3d).

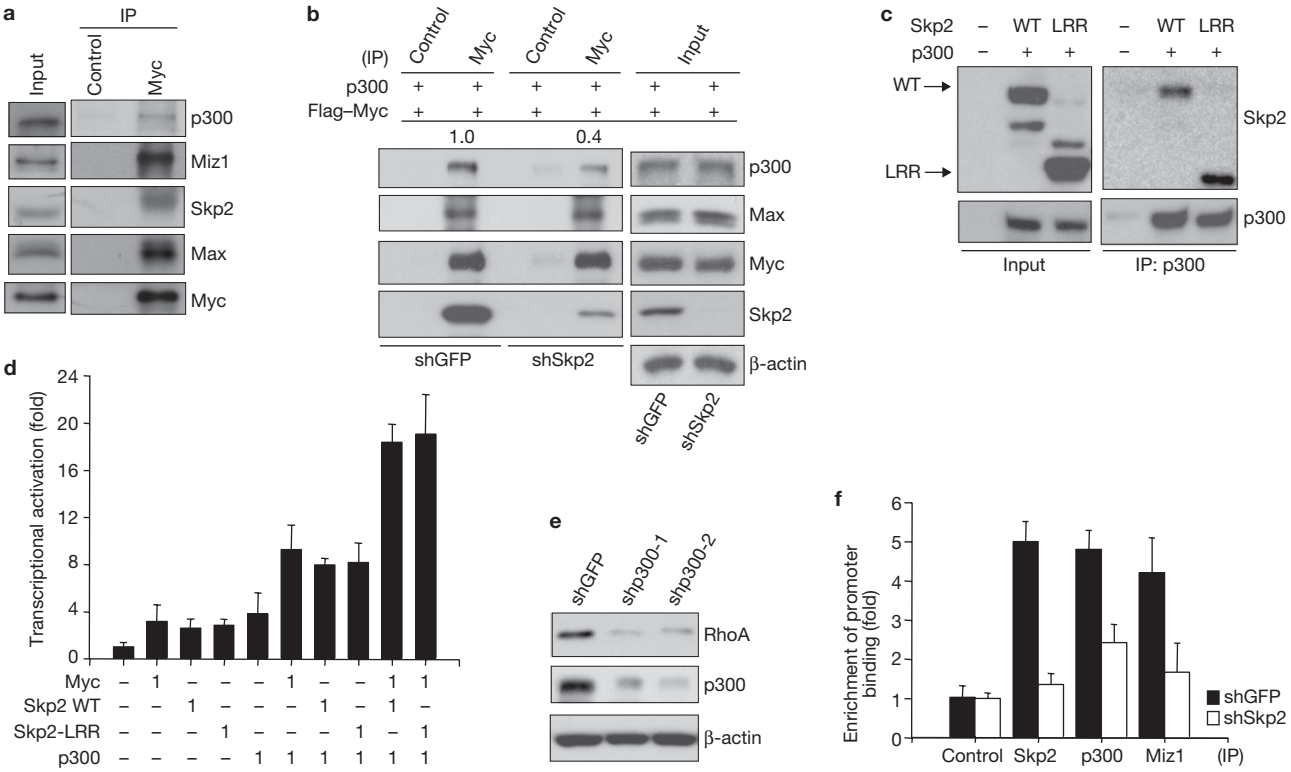

Figure 5 Skp2 cooperates with Myc to regulate *RhoA* transcription by recruiting p300. (**a**) Endogenous Myc interacts with endogenous p300, Miz1, Skp2 and Max *in vivo*. 293T total cell lysates were immunoprecipitated (IP) with Myc antibody, followed by western blot analysis. (**b**) Co-immunoprecipitation assay in 293T cells with GFP or Skp2 knockdown. The relative intensities of p300 were quantified with ImageQuant software and normalized with the levels of immunoprecipitated Myc in GFP or Skp2-silenced cells. (**c**) Co-immunoprecipitation assay in 293T cells transfected with the indicated plasmids. (**d**) RhoA reporter assay in 293T cells transfected with the indicated plasmids. The number indicates the amount (μg) of the plasmids used in this assay. The results are shown as means and s.d. of one representative experiment (from three independent experiments) performed in triplicate. (**e**) Western blot analysis of p300 and RhoA expression in MDA-MB-231 cells with GFP or p300 knockdown. Two p300 lentiviral shRNAs were used in this assay. (**f**) ChIP assay in PC-3 cells with GFP or Skp2 knockdown followed by real-time PCR analysis with various antibodies for immunoprecipitation as indicated. The quantified results are presented as means ± s.d. ($n = 3$). Uncropped images of blots are shown in Supplementary Information, Fig. S11.

Although Myc induced *RhoA* transcriptional activation in green fluorescent protein (GFP)-knockdown cells, it failed to activate *RhoA* transcription in Skp2-knockdown cells (Fig. 3e), suggesting that Skp2 is required for Myc-mediated *RhoA* transcription. Consistent with the role of Skp2 in *RhoA* transcription was our finding that *Skp2*$^{-/-}$ MEFs showed a profound decrease in *RhoA* mRNA levels, RhoA protein levels and RhoA activity (Fig. 3f, g). Similarly, Skp2 knockdown markedly decreased RhoA levels, whereas Skp2 overexpression induced RhoA protein expression (Fig. 3h, i; Supplementary Information, Fig. S5a, b). Our results therefore underscore the critical role of the Myc and Skp2 network in *RhoA* transcription and suggest that SCF–Skp2 E3 ligase activity is not required for this function.

Skp2 regulates cell migration and invasion by affecting RhoA expression

Skp2 overexpression is associated with cancer progression and metastasis[33,34], suggesting that Skp2 may be important in cancer cell migration, invasion and metastasis. Indeed, we observed that *Skp2*$^{-/-}$ MEFs or Skp2-knockdown cells showed a marked decrease in cell migration and invasion (Fig. 4a–c; Supplementary Information, Fig. S5c, d), recapitulating the phenotypes in Myc-knockdown and RhoA-knockdown cells (Fig. 2d, f; Supplementary Information, Fig. S1e, g). The effect of *Skp2* deficiency on cell migration and invasion was not due to its ability to regulate cell proliferation and apoptosis, because Skp2 knockdown did not significantly affect either cell proliferation or apoptosis within 2 days (Supplementary Information, Fig. S2a, c). However, Skp2 knockdown inhibited cell proliferation at later time points and also primary tumour formation (Supplementary Information, Fig. S2a, d), supporting its oncogenic activity[30,31,34]. Similarly, Skp2 overexpression markedly promoted cell migration in the same way as Myc and RhoA overexpression did (Fig. 4d; Supplementary Information, Fig. S1h, i). Restoration of RhoA expression rescued both cell migration and invasion defects in *Skp2*$^{-/-}$ MEFs and Skp2-knockdown cells (Fig. 4a; Supplementary Information, Fig. S5c, e), suggesting that RhoA serves as a critical downstream effector for Myc and Skp2 in cell migration and invasion. The restoration of the Skp2-LRR mutant also rescued RhoA protein expression and the cell invasion defect in *Skp2*$^{-/-}$ MEFs in the same way as wild-type Skp2 did (Fig. 4e). Our results therefore suggest a novel E3 ligase-independent function for Skp2 in *RhoA* transcription and cell invasion.

Skp2 recruits p300 and Miz1 to the Myc transcriptional complex to induce *RhoA* transcription

Because Skp2 is required for Myc-mediated *RhoA* transcription in an SCF E3 ligase-independent manner, it is very likely that Skp2 interacts

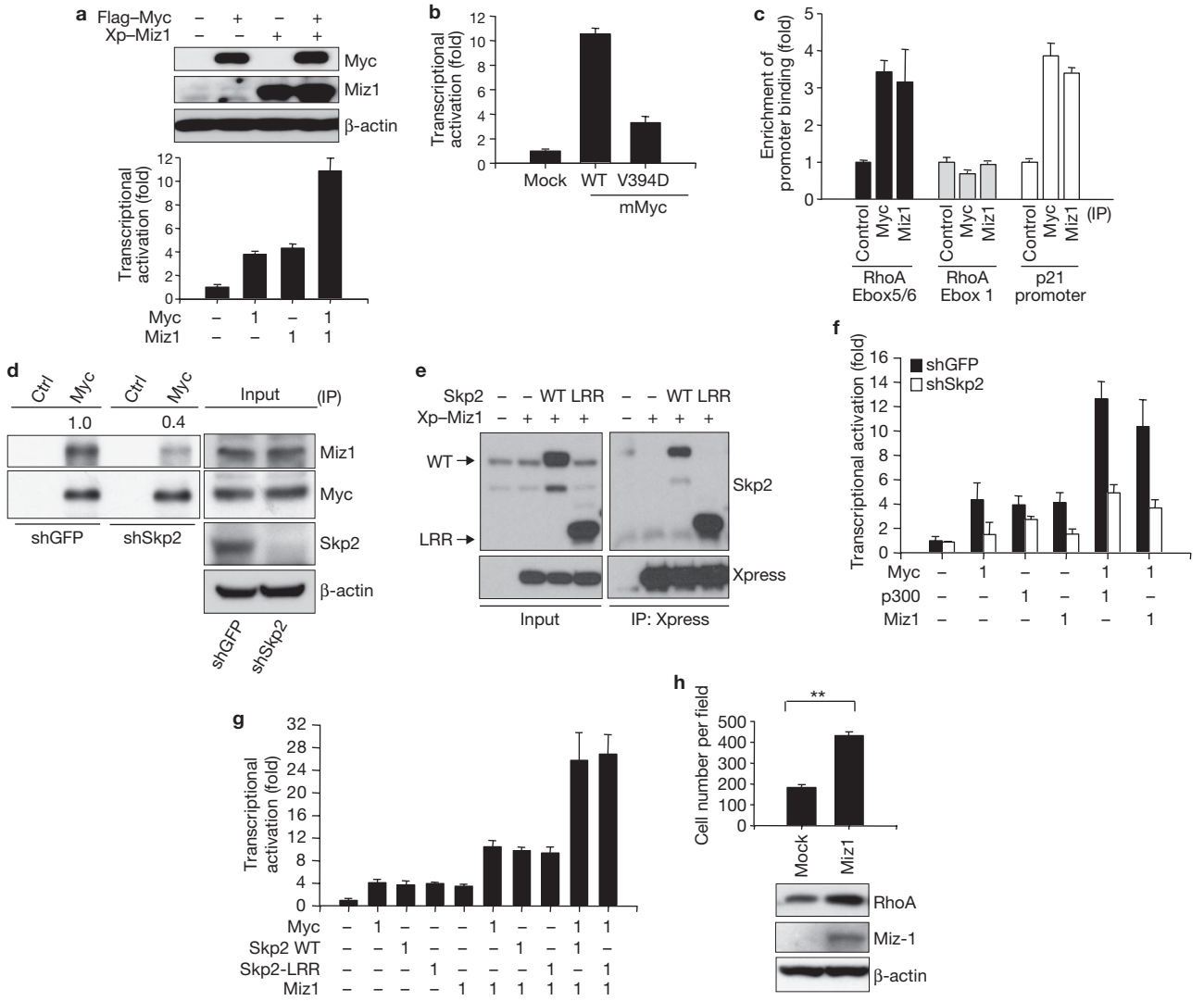

Figure 6 Skp2 cooperates with Myc to regulate *RhoA* transcription by recruiting Miz1. (**a**) RhoA reporter assay and western blot analysis in 293T cells transfected with the indicated plasmids. The numbers in the lower panel indicate the amount (μg) of each plasmid used in this assay. Upper panel: western blot analysis showing the expression of constructs as indicated. (**b**) The effect of MycV394D mutant on *RhoA* transcription. RhoA reporter assay in 293T cells transfected with the mouse WT Myc and MycV394D mutant. (**c**) ChIP assay in PC-3 cells followed by real-time PCR analysis using various antibodies for immunoprecipitation as indicated. The quantified results are presented as means ± s.d. ($n = 3$). (**d**) Endogenous immunoprecipitation assay in 293T cells with GFP or Skp2 knockdown. The relative intensity of Miz1 was quantified with ImageQuant software and normalized with the levels of immunoprecipitated Myc in GFP-silenced or Skp2-silenced cells. (**e**) Co-immunoprecipitation assay in 293T cells transfected with the indicated plasmids. (**f**) RhoA reporter assay in 293T cells with GFP or Skp2 knockdown transfected with plasmids as indicated. (**g**) RhoA reporter assay in 293T cells transfected with the indicated plasmids. (**h**) Matrigel cell invasion assay and western blot analysis in MDA-MB-231 cells infected with MSCV or MSCV-Miz1. The quantified results are presented as means ± s.d. ($n = 4$). Results in **a**, **b**, **f** and **g** are shown as means ± s.d. of one representative experiment (from three independent experiments) performed in triplicate. Uncropped images of blots are shown in Supplementary Information, Fig. S11.

with other co-regulators and recruits them to the Myc transcriptional complex for RhoA activation. p300 is known to serve as a coactivator for Myc on numerous Myc target genes, and the interaction between p300 and Skp2 has recently been unravelled[35]. To gain further insight into how Skp2 regulates *RhoA* transcription, we determined whether Skp2 interacts with p300 and recruits p300 to the Myc transcriptional complex. We found that Skp2 interacted with Myc and p300, and the Myc immunocomplex contained both Skp2 and p300 (Supplementary Information, Fig. S6a–c). The endogenous Myc complex also consisted of Skp2, p300 and Max, and the presence of these proteins in the Myc immunocomplex was decreased on Myc knockdown (Fig. 5a; Supplementary Information, Fig. S6d), suggesting that Myc forms a complex with Skp2, p300 and Max. Skp2 knockdown significantly decreased the interaction between Myc and p300 but not that between Myc and Max (Fig. 5b).

As expected, we found that Skp2-LRR interacted with Myc and p300 and cooperated with them to activate *RhoA* transcription in the same way as wild-type Skp2 did (Fig. 5c, d; Supplementary Information, Fig. S6d). p300 could induce, and synergized with, Myc and Skp2 to activate *RhoA* transcription, whereas its knockdown profoundly

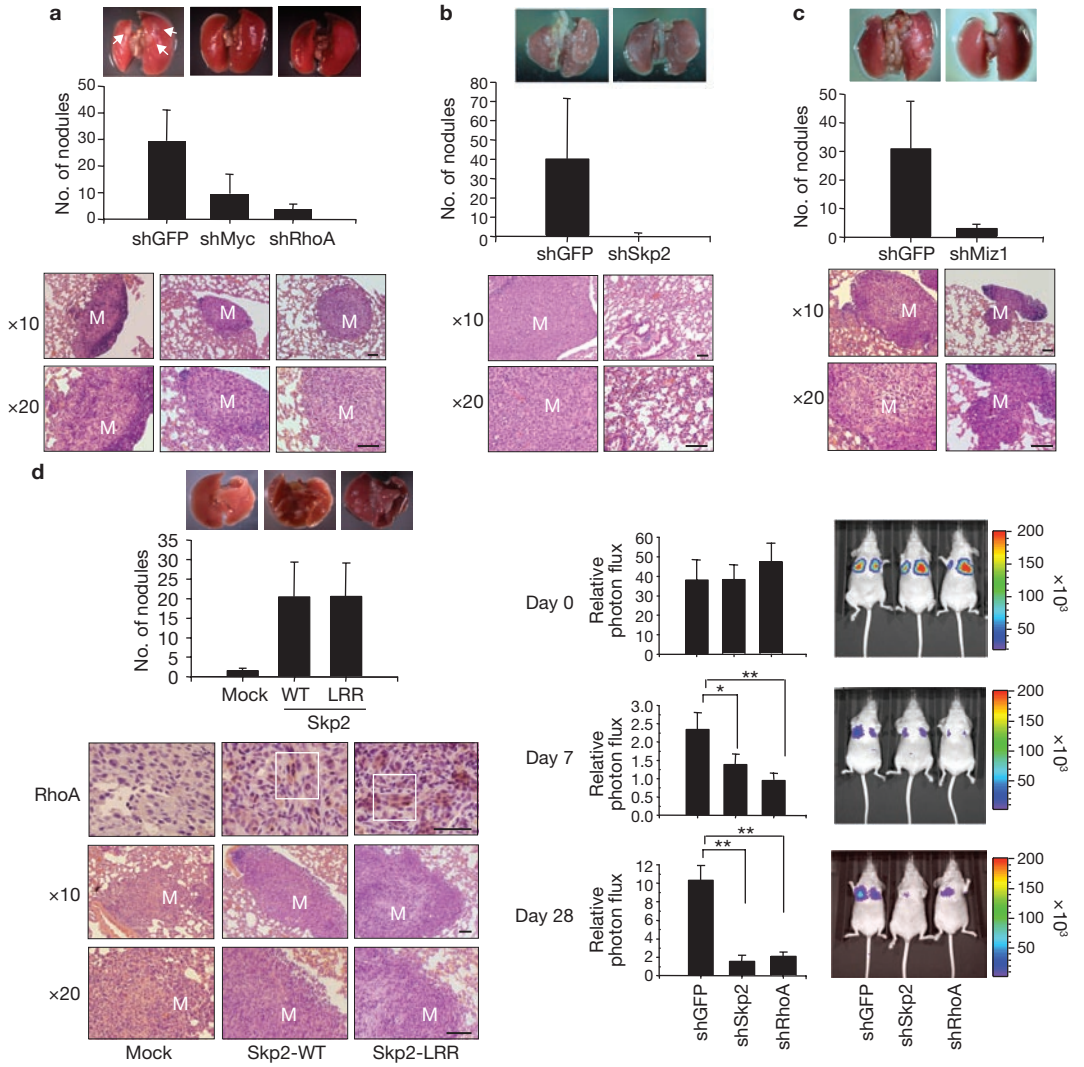

Figure 7 The Myc–Skp2–Miz1 complex regulates cancer metastasis in mouse model. (**a**–**c**) Lung metastasis assay and histological analysis from nude mice injected with MDA-MB-231 cells with GFP, Myc, RhoA (**a**), Skp2 (**b**) or Miz1. (**c**) knockdown; $n = 6$ for each group. M, metastatic nodule. Arrows in **a** indicate lung nodules. (**d**) Lung metastasis assay and histological analysis from nude mice injected with MDA-MB-231 cells infected with pBabe, pBabe-Skp2 WT or pBabe-Skp2-LRR. IHC of RhoA protein expression in metastatic breast tumour in the lung obtained from nude mice injected with MDA-MB-231 cells with pBabe, pBabe-Skp2 WT or pBabe-Skp2-LRR; $n = 5$ for each group. The white box indicates that RhoA protein expression was enhanced. (**e**) MDA-MB-231-Luc cells with GFP, Skp2 or RhoA knockdown were injected into nude mice, and the kinetics of breast cancer metastasis to the lung was measured by bioluminescence and quantified. Representative bioluminescent images are shown for days 0, 7 and 28. The results are presented as means ± s.d. ($n = 7$ for each group). Asterisk, $P < 0.05$; two asterisks, $P < 0.01$. Scale bar, 100 μm.

decreased RhoA protein expression (Fig. 5d, e). The ChIP assay revealed that endogenous p300 was also present in the *RhoA* promoter, and the recruitment of p300 to the *RhoA* promoter was impaired in Skp2-knockdown cells (Fig. 5f; Supplementary Fig. S6e). These results support the notion that Skp2 recruits p300 to the Myc complex to activate *RhoA* transcription independently of its SCF E3 ligase activity.

Miz1 was originally identified as a Myc-interacting protein that causes cell growth arrest by inducing expression of the cell-cycle inhibitors p15 and p21 (refs 36–38). In line with these reports[36–38], we found that Miz1 knockdown promoted cancer cell growth (Supplementary Information, Fig. S2b). We examined the effect of Miz1 on Myc-mediated *RhoA* transcription. We found that that Miz1 induced and synergized with Myc to activate *RhoA* transcription (Fig. 6a). To further support the role of Miz1 in Myc-mediated *RhoA* transcription, we used the V394D mutant of Myc, which is defective in Miz1 binding, for the *RhoA* transcription assay[39]. MycV394D compromised the ability of Myc to induce *RhoA* transcription (Fig. 6b; Supplementary Information, Fig. S6f, g), suggesting that Miz1 is important in Myc-mediated *RhoA* transcription.

The ChIP assay revealed that endogenous Miz1 was also present in the same *RhoA* promoter as Myc, Max, Skp2 and p300 (Figs 1d, 3c and 6c; Supplementary Information, Fig. S6e). As a control, we showed that Miz1, like Myc, was present in the p21 core promoter region[39] but not in the distal E-box1 region of the *RhoA* promoter (Fig. 6c). Endogenous Miz1 was also present in the endogenous Myc–Skp2–p300 immunocomplex (Fig. 5a). The recruitment of Miz1 to the Myc complex and the *RhoA* promoter relied partly on Skp2, because Skp2 knockdown decreased the ability of Miz1 to interact with Myc and its binding to the *RhoA* promoter (Figs 5f and 6d). This result was partly explained by the fact that Skp2 was able to interact with

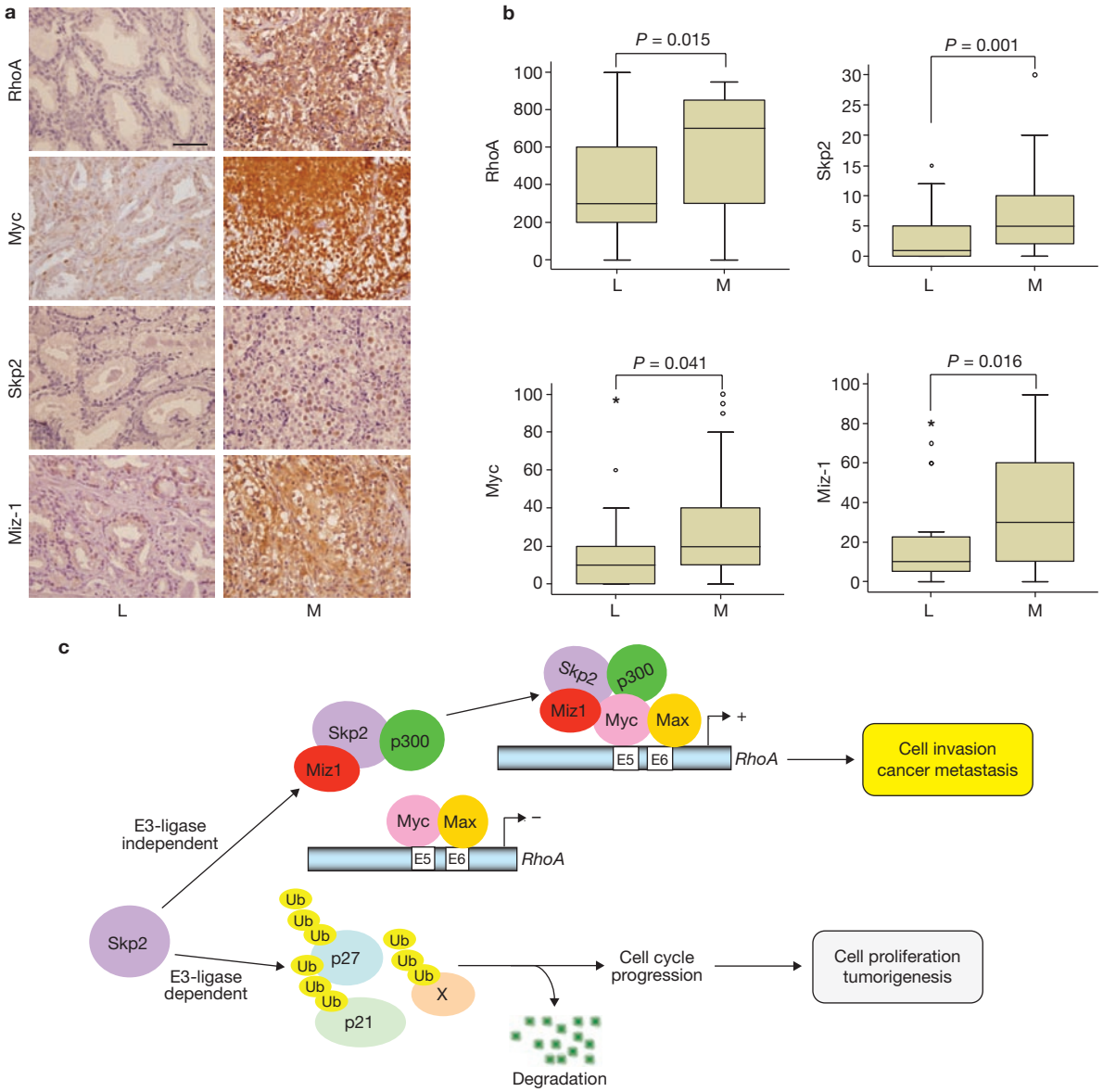

Figure 8 The Myc–Skp2–Miz1 complex is overexpressed and correlated with RhoA expression in metastatic prostate cancer samples. (**a**) The expression of RhoA, Myc, Skp2 and Miz1 in representative cases of primary prostate adenocarcinomas that remained localized (L) or developed metastasis (M). The labelling indices of RhoA, Myc, Skp2 and Miz1 appeared lower in the localized tumour but indicated significant overexpression in the case with metastasis. Original magnification, ×400. Scale bar, 100 μm. (**b**) The expression of RhoA, Myc, Skp2 and Miz1 in primary prostate cancer versus metastatic prostate cancer. Boxes indicate interquartile range. Bars from each box extend to largest and smallest observations. Data not included between the whiskers are plotted as minor (open circles) or major (asterisk) outliers. (**c**) The working model for SCF–Skp2 E3 ligase-dependent and ligase-independent functions.

Miz1 (Fig. 6e). As a consequence, *RhoA* transcriptional activation induced by Myc, Miz1 and p300 was impaired in Skp2-knockdown cells (Fig. 6f). Similarly, we found that the synergetic effect of Myc with p300 or Miz1 on *RhoA* transcription was diminished on Skp2 knockdown (Fig. 6f).

The Skp2-LRR mutant interacted with Miz1 and synergized with Miz1 and Myc to induce *RhoA* transcription in the same way as wild-type Skp2 did (Fig. 6e, g). Similarly, Miz1 overexpression induced RhoA protein expression, whereas its knockdown decreased it (Fig. 6h; Supplementary Information, Fig. S6h). Despite the fact that Miz1 overexpression causes cell-cycle arrest[36–38], it promoted cell invasion (Fig. 6g). Our results therefore support the notion that Skp2 induces *RhoA* transcription, cell migration and cell invasion by recruiting p300 and Miz1 to the Myc complex independently of its SCF–Skp2 E3 ligase activity.

The Myc–Skp2–Miz1 complex is critical for cancer metastasis

We used a well-established metastasis animal model to determine the role of the Myc–Skp2–Miz1 complex and RhoA in breast cancer metastasis[40–42]. Deficiency of Myc or Skp2 profoundly restricted breast cancer metastasis to the lung, whereas overexpression of Myc or Skp2 promoted it (Fig. 7a, b, d; Supplementary Information, Fig. S7a). Although Miz1 is thought to be a tumour suppressor whose knockdown enhances cell proliferation (Supplementary Information, Fig. S2b), Miz1 knockdown significantly suppressed cancer metastasis to the lung (Fig. 7c). RhoA deficiency phenocopied metastasis defects in the knockdown of the Myc–Skp2–Miz1 complex (Fig. 7a). Deficiency of Myc, Skp2 or Miz1 consistently decreased RhoA protein expression in metastatic breast tumours within the lung, whereas overexpression of

Myc or Skp2 enhanced it (Fig. 7d; Supplementary Information, Fig. S7). Our results underscore the critical role of the Myc–Skp2–Miz1 complex in RhoA expression, cell invasion and cancer metastasis.

We next determined whether Skp2 also shows SCF–Skp2 E3 ligase-independent function in cancer metastasis. Skp2-LRR strikingly promoted breast cancer metastasis to the lung in the same way as wild-type Skp2 did, which correlated with its ability to induce RhoA expression in metastatic breast tumours in the lung (Fig. 7d). However, Skp2-LRR compromised its effects on promoting cell-cycle progression, cell proliferation and primary tumour formation compared with wild-type Skp2 (Supplementary Information, Fig. S8), supporting the current view of the SCF–Skp2 E3 ligase-dependent role in cell-cycle progression and tumorigenesis[30,31,34]. Accordingly, our results strongly support a novel SCF–Skp2 E3 ligase-independent role in cancer metastasis.

To gain further insight into how Skp2 regulates cancer metastasis, we monitored the kinetics of breast cancer metastasis to the lung by using bioluminescence imaging. We found that the circulation of breast cancer cells with control or Skp2 silencing to the lung was comparable 2 h (day 0) after the injection into the tail vein (Fig. 7e), suggesting that Skp2 does not affect the arrival of breast cancer cells to the lung. However, the bioluminescence signal in the lung was decreased in Skp2 knockdown cells within the first week, and the profound decrease in bioluminescence signal was also observed at later time points (Fig. 7e; Supplementary Information, Fig. S9), indicating that Skp2 positively regulates the colonization of breast cancer cells in the lung and subsequent metastasis there. In support of the role of Skp2 in RhoA expression and cancer metastasis, we found that RhoA knockdown phenocopied the effects of Skp2 knockdown on these processes (Fig. 7e; Supplementary Information, Fig. S9). These results suggest that Skp2 and RhoA affect the colonization of breast cancer cells in the lung, in turn regulating cancer metastasis.

The Myc–Skp2–Miz1 complex is overexpressed and correlated with RhoA expression in metastatic human cancers

Because Myc–Skp2–Miz1 overexpression is correlated with RhoA expression *in vitro* and these components are critical for cancer metastasis, we sought to determine whether there is a positive correlation between RhoA expression and the Myc–Skp2–Miz1 complex in human cancer samples. Analysing prostate cancer samples (64 cases), we found that the expression of RhoA ($P = 0.015$), Myc ($P = 0.041$), Skp2 ($P = 0.001$) and Miz1 ($P = 0.016$) was significantly correlated with prostate cancer metastasis compared with primary prostate cancer (Fig. 8a, b; Supplementary Information, Fig. S10a). RhoA expression was also significantly correlated with Myc ($P = 0.024$), Skp2 ($P = 0.007$) and Miz1 ($P < 0.001$) in prostate cancers (Supplementary Information, Fig. S10b). We found that there was also a positive correlation between the components of the Myc–Skp2–Miz1 complex (for example Myc and Skp2 ($P = 0.001$), Myc and Miz1 ($P < 0.001$) and Skp2 and Miz1 ($P < 0.001$); Supplementary Information, Fig. S10b). Our study therefore underscores the clinical relevance of the Myc–Skp2–Miz1 complex and RhoA expression in cancer metastasis.

DISCUSSION

Our study provides the first clue as to how *RhoA* transcription is induced. We found that *RhoA* transcription is orchestrated by the Myc–Skp2–Miz1–p300 transcriptional complex. Knockdown or deficiency of these components impairs RhoA expression, resulting in defects in cell migration and invasion. This finding is further underscored by the important clinical observations that RhoA expression was positively correlated with the Myc–Skp2–Miz1 complex in metastatic prostate cancer, which may provide the relevant molecular mechanism by which RhoA overexpression occurs during cancer progression and metastasis.

Myc ubiquitylation by HectH9 and Skp2 has been shown to be critical for Myc target genes involved in cell-cycle progression and proliferation[18–20]. However, our study suggests that Myc ubiquitylation by these two E3 ligases is not required for *RhoA* gene expression. Although Myc is thought to display an oncogenic activity partly through antagonizing Miz1 transcriptional activity towards p21 and p15 gene expression, it has been unclear whether Miz1 has any impact on Myc transcriptional activation. The current dogma favours the notion of a mutual antagonism between the oncogenic Myc and the tumour suppressor Miz1 in gene regulation[15–17,43]. Our results show that Miz1 synergizes with Myc to induce *RhoA* transcription, providing a new insight into the novel regulatory mechanism between Myc and Miz1. Although Miz1 overexpression causes cell-cycle arrest and inhibits cell proliferation[36–38], we found that Miz1 cooperates with Myc to induce RhoA expression and cancer cell invasion and is required for cancer metastasis, which is consistent with our finding that Myc, Miz1 or RhoA overexpression are positively correlated with each other in metastatic cancer samples. Our study therefore reveals a previously unrecognized function of Miz1 in *RhoA* transcription, cell invasion and cancer metastasis.

Skp2 depends on SCF–Skp2 E3 ligase activity to exert its oncogenic activity towards the promotion of cell proliferation and tumorigenesis (Supplementary Information, Fig. S8)[30,31,34]. Our study reveals a SCF–Skp2 E3 ligase-independent function for Skp2 in *RhoA* transcription, cell invasion and cancer metastasis. We propose a novel SCF E3 ligase-independent function for Skp2: specifically, that Skp2 recruits Miz1 and p300 co-regulators to the Myc complex, in turn facilitating *RhoA* transcription, cell invasion and cancer metastasis (Fig. 8c). In contrast, SCF–Skp2 E3 ligase is required for the functioning of Skp2 in cell-cycle progression, proliferation and primary tumour formation by promoting the ubiquitylation and degradation of its substrates such as p27.

Our study reveals that the Myc–Skp2–Miz1 transcriptional complex is critical for *RhoA* transcription, cell migration and invasion, and cancer metastasis. Our findings, that overexpression of the Myc–Skp2–Miz1 complex promotes cancer cell invasion and metastasis whereas their deficiency restricts cancer metastasis, suggest that targeting this transcriptional complex may provide appealing therapeutic strategies for the treatment of cancer patients with metastasis. □

METHODS

Methods and any associated references are available in the online version of the paper at http://www.nature.com/naturecellbiology/

Note: Supplementary Information is available on the Nature Cell Biology website.

ACKNOWLEDGEMENTS

We thank R. Weinberg, W. Sellers, D. Bohmann, W. Tansey, J. M. Sedivy, W. Wei, M. Pagano, M. Eilers, W. S. El-Deiry, L. Yao and D. Sarbassov for reagents. We also thank D. Sarbassov, M. H. Lee and M. G. Lee for comments and suggestions. Special thanks are extended to S. Patterson for editing and critical reading of the manuscript. This work was supported by Research Trust Scholar funds from the

M. D. Anderson Cancer Center, the National Cancer Institute's Prostate Cancer Specialized Program of Research Excellence (SPORE) at the M. D. Anderson Cancer Center, a Department of Defense Prostate Cancer New Investigator Award (to H.K.L.) and a grant from the Department of Health, Taiwan (to C.F.L.).

AUTHOR CONTRIBUTIONS

C.H.C. and H.K.L. designed the experiments and wrote the manuscript. C.H.C., H.K.L., S.W.L., J.W., W.L.Y., C.Y.W. and J.W. performed the experiments. H.Y.K., C.F.L. and H.Y.H. performed the immunochemistry and analysed the data. M.C.H. and P.P.P. provided the cell lines and reagents. K.I.N. provided the *Skp2*$^{-/-}$ mice.

COMPETING FINANCIAL INTERESTS

The authors declare no competing financial interests.

Published online at http://www.nature.com/naturecellbiology
Reprints and permissions information is available online at http://npg.nature.com/reprintsandpermissions/

1. Chiang, A. C. & Massagué, J. Molecular basis of metastasis. *N. Engl. J. Med.* **359,** 2814–2823 (2008).
2. Yang, J. & Weinberg, R. A. Epithelial–mesenchymal transition: at the crossroads of development and tumor metastasis. *Dev. Cell* **14,** 818–829 (2008).
3. Jaffe, A. B. & Hall, A. Rho GTPases: biochemistry and biology. *Annu. Rev. Cell Dev. Biol.* **21,** 247–269 (2005).
4. Lahoz, A. & Hall, A. DLC1: a significant GAP in the cancer genome. *Genes Dev.* **22,** 1724–1730 (2008).
5. Moscow, J. A. *et al.* Examination of human tumors for rhoA mutations. *Oncogene* **9,** 189–194 (1994).
6. Rihet, S. *et al.* Mutation status of genes encoding RhoA, Rac1, and Cdc42 GTPases in a panel of invasive human colorectal and breast tumors. *J Cancer Res. Clin. Oncol.* **127,** 733–738 (2001).
7. Bellizzi, A. *et al.* RhoA protein expression in primary breast cancers and matched lymphocytes is associated with progression of the disease. *Int. J. Mol. Med.* **22,** 25–31 (2008).
8. Faried, A., Faried, L. S., Usman, N., Kato, H. & Kuwano, H. Clinical and prognostic significance of RhoA and RhoC gene expression in esophageal squamous cell carcinoma. *Ann. Surg. Oncol.* **14,** 3593–3601 (2007).
9. Horiuchi, A. *et al.* Up-regulation of small GTPases, RhoA and RhoC, is associated with tumor progression in ovarian carcinoma. *Lab. Invest.* **83,** 861–870 (2003).
10. Zhao, X. *et al.* Overexpression of RhoA induces preneoplastic transformation of primary mammary epithelial cells. *Cancer Res.* **69,** 483–491 (2009).
11. Pille, J. Y. *et al.* Anti-RhoA and anti-RhoC siRNAs inhibit the proliferation and invasiveness of MDA-MB-231 breast cancer cells in vitro and in vivo. *Mol. Ther.* **11,** 267–274 (2005).
12. Valastyan, S. *et al.* A pleiotropically acting microRNA, miR-31, inhibits breast cancer metastasis. *Cell* **137,** 1032–1046 (2009).
13. Kamai, T. *et al.* RhoA is associated with invasion and lymph node metastasis in upper urinary tract cancer. *Br. J. Urol. Int.* **91,** 234–238 (2003).
14. Faried, A. *et al.* Correlation between RhoA overexpression and tumour progression in esophageal squamous cell carcinoma. *Eur. J. Surg. Oncol.* **31,** 410–414 (2005).
15. Kleine-Kohlbrecher, D., Adhikary, S. & Eilers, M. Mechanisms of transcriptional repression by Myc. *Curr. Top. Microbiol. Immunol.* **302,** 51–62 (2006).
16. Adhikary, S. & Eilers, M. Transcriptional regulation and transformation by Myc proteins. *Nature Rev. Mol. Cell Biol.* **6,** 635–645 (2005).
17. Eilers, M. & Eisenman, R. N. Myc's broad reach. *Genes Dev.* **22,** 2755–2766 (2008).
18. Adhikary, S. *et al.* The ubiquitin ligase HectH9 regulates transcriptional activation by Myc and is essential for tumor cell proliferation. *Cell* **123,** 409–421 (2005).
19. Kim, S. Y., Herbst, A., Tworkowski, K. A., Salghetti, S. E. & Tansey, W. P. Skp2 regulates Myc protein stability and activity. *Mol. Cell* **11,** 1177–1188 (2003).
20. von der Lehr, N. *et al.* The F-box protein Skp2 participates in c-Myc proteosomal degradation and acts as a cofactor for c-Myc-regulated transcription. *Mol. Cell* **11,** 1189–1200 (2003).
21. Ansieau, S. *et al.* Induction of EMT by twist proteins as a collateral effect of tumor-promoting inactivation of premature senescence. *Cancer Cell* **14,** 79–89 (2008).
22. Smit, M. A. & Peeper, D. S. Deregulating EMT and senescence: double impact by a single twist. *Cancer Cell* **14,** 5–7 (2008).
23. Meyer, N. & Penn, L. Z. Reflecting on 25 years with MYC. *Nature Rev. Cancer* **8,** 976–990 (2008).
24. Prochownik, E. V. c-Myc: linking transformation and genomic instability. *Curr. Mol. Med.* **8,** 446–458 (2008).
25. Ricci, M. S. *et al.* Direct repression of FLIP expression by c-myc is a major determinant of TRAIL sensitivity. *Mol. Cell. Biol.* **24,** 8541–8555 (2004).
26. Frank, S. R., Schroeder, M., Fernandez, P., Taubert, S. & Amati, B. Binding of c-Myc to chromatin mediates mitogen-induced acetylation of histone H4 and gene activation. *Genes Dev.* **15,** 2069–2082 (2001).
27. Bello-Fernandez, C., Packham, G. & Cleveland, J. L. The ornithine decarboxylase gene is a transcriptional target of c-Myc. *Proc. Natl Acad. Sci. USA* **90,** 7804–7808 (1993).
28. Kaiser, P., Flick, K., Wittenberg, C. & Reed, S. I. Regulation of transcription by ubiquitination without proteolysis: Cdc34/SCF^{Met30}-mediated inactivation of the transcription factor Met4. *Cell* **102,** 303–314 (2000).
29. Bres, V. *et al.* A non-proteolytic role for ubiquitin in Tat-mediated transactivation of the HIV-1 promoter. *Nature Cell Biol.* **5,** 754–761 (2003).
30. Frescas, D. & Pagano, M. Deregulated proteolysis by the F-box proteins SKP2 and β-TrCP: tipping the scales of cancer. *Nature Rev. Cancer* **8,** 438–449 (2008).
31. Nakayama, K. I. & Nakayama, K. Regulation of the cell cycle by SCF-type ubiquitin ligases. *Semin. Cell Dev. Biol.* **16,** 323–333 (2005).
32. Liu, Y. *et al.* The ETS protein MEF is regulated by phosphorylation-dependent proteolysis via the protein-ubiquitin ligase SCF^{Skp2}. *Mol. Cell. Biol.* **26,** 3114–3123 (2006).
33. Stanbrough, M. *et al.* Increased expression of genes converting adrenal androgens to testosterone in androgen-independent prostate cancer. *Cancer Res.* **66,** 2815–2825 (2006).
34. Lin, H. K. *et al.* Phosphorylation-dependent regulation of cytosolic localization and oncogenic function of Skp2 by Akt/PKB. *Nature Cell Biol.* **11,** 420–432 (2009).
35. Kitagawa, M., Lee, S. H. & McCormick, F. Skp2 suppresses p53-dependent apoptosis by inhibiting p300. *Mol. Cell* **29,** 217–231 (2008).
36. Seoane, J. *et al.* TGFβ influences Myc, Miz-1 and Smad to control the CDK inhibitor p15^{INK4b}. *Nature Cell Biol.* **3,** 400–408 (2001).
37. Staller, P. *et al.* Repression of p15^{INK4b} expression by Myc through association with Miz-1. *Nature Cell Biol.* **3,** 392–399 (2001).
38. Wanzel, M. *et al.* A ribosomal protein L23-nucleophosmin circuit coordinates Miz1 function with cell growth. *Nature Cell Biol.* **10,** 1051–1061 (2008).
39. Wu, S. *et al.* Myc represses differentiation-induced p21^{CIP1} expression via Miz-1-dependent interaction with the p21 core promoter. *Oncogene* **22,** 351–360 (2003).
40. Gupta, G. P. *et al.* Mediators of vascular remodelling co-opted for sequential steps in lung metastasis. *Nature* **446,** 765–770 (2007).
41. Wu, Y. *et al.* Stabilization of snail by NF-κB is required for inflammation-induced cell migration and invasion. *Cancer Cell* **15,** 416–428 (2009).
42. Gupta, G. P. *et al.* ID genes mediate tumor reinitiation during breast cancer lung metastasis. *Proc. Natl Acad. Sci. USA* **104,** 19506–19511 (2007).
43. Wanzel, M., Herold, S. & Eilers, M. Transcriptional repression by Myc. *Trends Cell Biol.* **13,** 146–150 (2003).

DOI: 10.1038/ncb2047

METHODS

Mice, cell culture and reagents. Mouse embryonic fibroblasts (MEFs) from wild-type and *Skp2*$^{-/-}$ mice were prepared as described previously. 293T, PC-3 (from ATCC), MDA-MB-231 and Rat1 cells (from M. J. M. Sedivy) were cultured in DMEM medium containing 10% fetal bovine serum (FBS). To clone Xp-Skp2, Skp2 was amplified by PCR using pcDNA3-Skp2 as a template and inserted into a pcDNA4–HisMax-TOPO vector (Invitrogen). To clone the full-length *RhoA* promoter, human *RhoA* promoter cDNA (nucleotides −1850 to +1, numbered relative to the transcription initiation site) was amplified from the genomic DNA of 293T cells and inserted into the pGL3 luciferase vector. The mutant *RhoA* promoters were generated by using the site-directed mutagenesis kit (Stratagene) in accordance with the manufacturer's standard procedure with the full-length *RhoA* promoter as a template. pBabe-Skp2 was generated by subcloning Skp2 into the *Eco*RI site of the pBabe vector. MSCV-PIG-RhoA and MSCV-Myc were generated by subcloning RhoA and c-Myc into the MSCV-PIG vector. His_6–ubiquitin and haemagglutinin (HA)–p27 constructs were from D. Bohmann (University of Rochester Medical Center, New York, USA) and M. Pagano (New York University Cancer Institute, USA), respectively. Myc-Twist and pcDNA-p300 were obtained from R. Weinberg (Massachusetts Institute of Technology, Boston, USA) and W. Sellers (Novartis Institutes for BioMedical Research, Cambridge, USA), respectively. HectH9 and the Skp2-LRR mutant were obtained from M. Eliers (University of Würzburg, Germany) and W. Tansey (Vanderbilt University Medical Centre, Tennessee, USA) respectively. pBabe-MycER and mouse pcDNA3.1-c-MycV394D were obtained from W. El-Deiry (University of Pennsylvania School of Medicine, Philadelphia, USA) and Libo Yao (State Key Laboratory of Cancer Biology, The Fourth Military Medical University, Xi'an, China), respectively. To clone Xp-Miz1, the human Skp2 cDNA was amplified by reverse transcriptase PCR (RT–PCR) from 293T cells and inserted into the pcDNA4–HisMax-TOPO vector. MG-132 was obtained from Calbiochem.

RhoA reporter assay. 293T cells were transfected by using Lipofectamine 2000 (Invitrogen) for 48 h, and luciferase activity was measured by using the dual luciferase system (Promega). Each sample was analysed in triplicate and experiments were performed at least three times. The relative luciferase activity was calculated as a ratio between firefly luciferase activity and *Renilla* luciferase activity.

Immunoprecipitation and immunoblotting. Immunoprecipitation (IP) and immunoblotting (IB) were performed essentially as described previously with some modifications. For protein–protein interaction, cells were lysed in E1A lysis buffer (250 mM NaCl, 50 mM HEPES pH 7.5, 0.1% Nonidet P40, 5 mM EDTA) containing a protease inhibitor cocktail (Roche). The following antibodies were used for IP, IB or immunofluorescence (IF): anti-Skp2 (IP, 1:250 dilution; IB, 1:1,000; Zymed), anti-Skp2 (IB, 1:1,000; Santa Cruz), anti-Skp1 (IB, 1:2,000; BD Transduction Lab), anti-Cul-1 (IB, 1:2,000; BD Transduction Lab), anti-Xpress (IP and IF, 1:500; IB, 1:5,000; Invitrogen), anti-HA (IB and IF, 1:1,000; Covance, Upstate), anti-β-actin (IB, 1:1,000; Sigma), anti-p27 (IP, 1:100; IB, 1:1,000; BD Transduction Lab), anti-Myc (IP, 1:100; IB, 1:1,000; Santa Cruz), anti-p300 (IP, 1:100; IB, 1:1,000; Santa Cruz), anti-Miz1 (IP, 1:100; IB, 1:1,000; Santa Cruz), anti-HectH9 (IB, 1:1,000; Abcam) and anti-RhoA (IB, 1:2,000; Santa Cruz).

RhoA activity assay. RhoA activity assay was performed with the use of a Rho activation assay kit (Millipore) in accordance with the manufacturer's instructions. Equal amounts of protein were used to pull down active Rho with glutathione *S*-transferase–Rhotekin Rho-binding domain, which binds selectively to GTP-Rho and not to GDP-Rho. After precipitation, samples were analysed by western blotting with a specific anti-RhoA antibody.

Viral infection. Retroviral plasmids were transfected into Phoenix packing cells for 2 days, and the virus-containing medium was harvested and used to infect target cells. For lentiviral shRNA infection, 293T cells were co-transfected with Skp2, Myc, RhoA or GFP control shRNA with packing plasmids (deltaVPR8.9) and envelope plasmid (VSV-G) using Lipofectamine 2000 reagent in accordance with the manufacturer's instructions. RhoA-lentiviral shRNA-1 (5′-GAAAGCAGGTAGAGTTGGCTT-3′), RhoA-lentiviral shRNA-2 (5′-GTACATGGAGTGTTCAGCAAA-3′), Skp2-lentiviral shRNA-1 (5′-GATAGTGTCATGCTAAAGAAT-3′), Skp2-lentiviral shRNA-2 (5′-GCCTAAGCTAAATCGAGAGAA-3′), Myc-lentiviral shRNA-1 (5′-CCTGAGACAGATCAGCAACAA-3′), Myc-lentiviral shRNA-2 (5′-CAGTTGAAACACAAACTTGAA-3′), p300-lentiviral shRNA-1 (5′-CAATTCCGAGACATCTTGAGA-3′), p300-lentiviral shRNA-2 (5′-CCAGCCTCAAACTACAATAAA-3′), Miz1-lentiviral shRNA-1 (5′-GTGTTCACTTTAAGGCTCATA-3′), Miz1-lentiviral shRNA-2 (5′-CGAGTACTTCAAGATGCTCTT-3′), HectH9-lentiviral shRNA-1 (5′-GCGTCTGTGTTGTGGAGGTTT-3′), HectH9-lentiviral shRNA-2 (5′-CCACACTTTCACAGATACTAT-3′), HectH9-lentiviral shRNA-3 (5′-GCTCCCACTATAACCTCACTT-3′), HectH9-lentiviral shRNA-4 (5′-CGACGAGAACTAGCACAGAAT-3′) and GFP shRNA (5′-GCAAGCTGACCCTGAAGTTC-3′) were transfected with packing plasmids into 293T cells for 2 days, and virus particles containing Skp2, Myc, RhoA or GFP shRNA were used to infect mammalian cells. All the infected cells were cultured in medium containing appropriate antibiotics.

ChIP assay. The ChIP assay was performed in accordance with the manufacturer's instructions (Upstate). A DNA–protein complex was sheared by sonication. A 1% portion of the sheared DNA–protein complex was kept as an input DNA sample. Anti-Skp2 (1:250, clone 8D9; Zymed), anti-Myc (1:100, clone N262; Santa Cruz), anti-Max (1:100, clone C17; Santa Cruz), anti-p300 (1:100, clone N15; Santa Cruz), anti-Miz1 (1:100, clone H190; Santa Cruz) and anti-RNA polymerase II (1:500, clone 6H5-3; Upstate) or normal mouse/rabbit IgG (1:500, Upstate and Sigma) were used for immunoprecipitation. Enrichment of promoter binding levels was analysed by real-time PCR, normalized by input, and expressed as a fold increase over the control. Primers used for real-time PCR were as follows: RhoA E-box5/6, 5′ -CTTCGCGTGCGTGAAGAGTTG-3′ and 5′-CATCCACTATTGCTCAGGAGC-3′ ; RhoA E-box1, 5′-GAGAAGCCTTCCCTGACCACC-3′ and 5′ -GCTCACTAATCAGGGCATTCAT-3′ ; p21 core promoter, 5′-ACCGGCTGGCCTGCTGGAACT-3′ and 5′ -TCTGCCGCCGCTCTCTCACCT-3′ . Quantified results are presented as means ± s.d.

***In vivo* ubiquitylation assay.** The *in vivo* ubiquitylation assay was performed as described[44]. In brief, 293T cells were transfected with the indicated plasmids for 24 h, treated with 20 μM MG-132 for 6 h, and lysed with denaturing buffer (6 M guanidine-HCl, 0.1 M Na_2HPO_4/NaH_2PO_4, 10 mM imidazole). The cell extracts were then incubated with nickel beads for 3 h, washed, and subjected to western blot analysis.

Cell migration and invasion assays. The cell migration assay was performed in a 24-well transwell plate with 8-μm polyethylene terephthalate membrane filters (Falcon cell culture insert; Becton-Dickinson) separating the lower and upper culture chambers. In brief, MEFs, MDA-MB-231 cells and PC-3 cells were plated in the upper chamber at 10^4, 5×10^4 and 10^5 cells per well, respectively, in serum-free DMEM. The bottom chamber contained DMEM with 10% FBS. MEFs and PC-3 cells were allowed to migrate for 18 h, whereas MDA-MB-231 cells were allowed to migrate for 6 h. After the incubation period, the filter was removed, and non-migrant cells on the upper side of the filter were detached with the use of a cotton swab. Filters were fixed with 4% formaldehyde for 15 min, and cells located in the lower filter were stained with 0.1% crystal violet for 20 min and three random fields were counted. Quantified results are presented as means ± s.d. The cell invasion assay was essentially similar to the cell migration assay, except that the membrane filter was precoated with diluted Matrigel (Matrigel:serum-free DMEM, 1:6) before the assay.

Immunohistochemistry and statistical analysis. Immunohistochemical analysis was performed on representative tissue blocks of primary prostatic adenocarcinomas from 64 patients. Among them, 37 patients presented with localized disease after follow-up for at least 5 years, and 27 patients developed metastatic disease either at diagnosis of adenocarcinoma or within 2 years. The sections were heated for epitope retrieval, quenched in 3% H_2O_2 to abolish endogenous peroxidase, and then incubated with 10% normal horse serum to block non-specific immunoreactivity. The primary antibodies were detected with an EnVision kit (Dako) for RhoA (26C4, 1:200; Santa Cruz Biotechnology), Myc (9E10, 1:200; Zymed Laboratories), Skp2 (2C8D9, 1:100; Zymed Laboratories) and Miz-1 (1:400; Atlas Antibodies). To evaluate the expression of all markers, the percentage of tumour cells with moderate or strong nuclear and/or cytoplasmic immunoreactivity was recorded to obtain the labelling index for each case. The correlations between the four markers were calculated by using Pearson's correlation test, and the differences in the labelling indices of the markers tested between cases with and without metastatic disease were compared by using Student's *t*-test.

Metastasis assay. To study RhoA, Myc, Skp2 or Miz1 deficiency in a breast cancer metastasis model, MDA-MB-231 cells silenced with GFP, RhoA, Myc, Skp2 or Miz1 lentiviral shRNAs were injected into the tail veins of athymic female nude mice. After 12 weeks, mice (n = 5–7 for each group) were killed and lung tissues were analysed for the occurrence of metastasis. To study the role of overexpression of Myc, wild-type Skp2 and Skp2-LRR in metastasis, MDA-MB-231 cells were infected with retroviruses expressing empty vector, Myc, Skp2 or Skp2-LRR and selected with 2 μg ml^{-1} puromycin for 4 days. These viable cells were injected into the tail vein of athymic male nude mice. Eight weeks later, mice (n = 6–7 for each group) were killed and lung tissues were obtained for analysis of cancer metastasis. To study the kinetics of breast cancer metastasis to the lung, MDA-MB-231-Luc cells stably overexpresssed with luciferase gene silenced with GFP, Skp2 or RhoA shRNA were injected into the lateral tail vein (2×10^6 cells) of athymic female nude mice (seven mice for each group). For bioluminescence imaging, mice were anaesthetized and given 150 mg g^{-1} D-luciferin in PBS by intraperitoneal injection. At 5 min after injection, bioluminescence was detected with an IVIS imaging system and analysed with Living Image software (Xenogen).

BrdU incorporation assay. BrdU incorporation assays were performed with the *in situ* cell proliferation kit, FLUOS (Roche). In brief, COS-1 cells transfected with various plasmids were serum-starved (0.1% FBS) for 24 h, refreshed with 10% FBS for 16 h, incubated with 20 μM bromodeoxyuridine (BrdU) for 1 h, and harvested for quantification of BrdU incorporation. The percentages of cell numbers in S phase were scored; representative images are shown as indicated (left panel), and quantitative results are presented as means ± s.d. (right panel).

Cell growth, apoptosis and *in vivo* tumorigenesis assay. For the cell growth assay, 5×10^3 cells were seeded in 12 wells in triplicate, harvested, and stained with trypan blue on different days. Viable cells were counted directly under the microscope. For the apoptosis assay, cells were cultured for 2 days, harvested, labelled with fluorescein isothiocyanate-tagged Annexin-V, and followed by flow cytometry analysis. For the *in vivo* tumorigenesis assay, cells were injected subcutaneously into athymic female nude mice, tumour size was measured weekly with a calliper, and tumour volume was determined with the standard formula $L \times W^2 \times 0.52$, where L is the longest diameter and W the shortest diameter.

Primer sequences for real-time RT–PCR. Human *CAD*, 5′-CAGGTTTGCCAGCTGAGGA-3′ (forward) and 5′-TGCCTGTCTCGGTACTGGTG-3′ (reverse); human *ODC*, 5′-TGTAGGAAGCGGCTGTAC-3′ (forward) and 5′-GCTATGATTCTCACTCCAGAG-3′ (reverse); human RhoA, 5′-GAGCACACAAGGCGGGAG-3′ (forward) and 5′-CTTGCAGAGCAGCTCTCGTAG-3′ (reverse); human GAPDH, 5′-GATTCCACCCATGGCAAATTC-3′ (forward) and 5′-CTTCTCCATGGTGGTGAAGAC-3′ (reverse); mouse RhoA, 5′-GAGTTGGCTTTATGGGACAC-3′ (forward) and 5′-GAAATGCTTGACTTCTGGAGTC-3′ (reverse); mouse GAPDH, 5′-GACAAAATGGTGAAGGTCGGTG-3′ (forward) and 5′--3′ (reverse).

Statistical analysis. Unless otherwise noted, data are presented as means ± s.d. of three or more independent results, and statistical significance was assessed by a two-tailed paired Student's t-test. $P < 0.05$ was considered significant.

44. Yang, W. L. *et al.* The E3 ligase TRAF6 regulates Akt ubiquitination and activation. *Science* **325,** 1134–1138 (2009).

nature cell biology

DOI: 10.1038/ncb2047

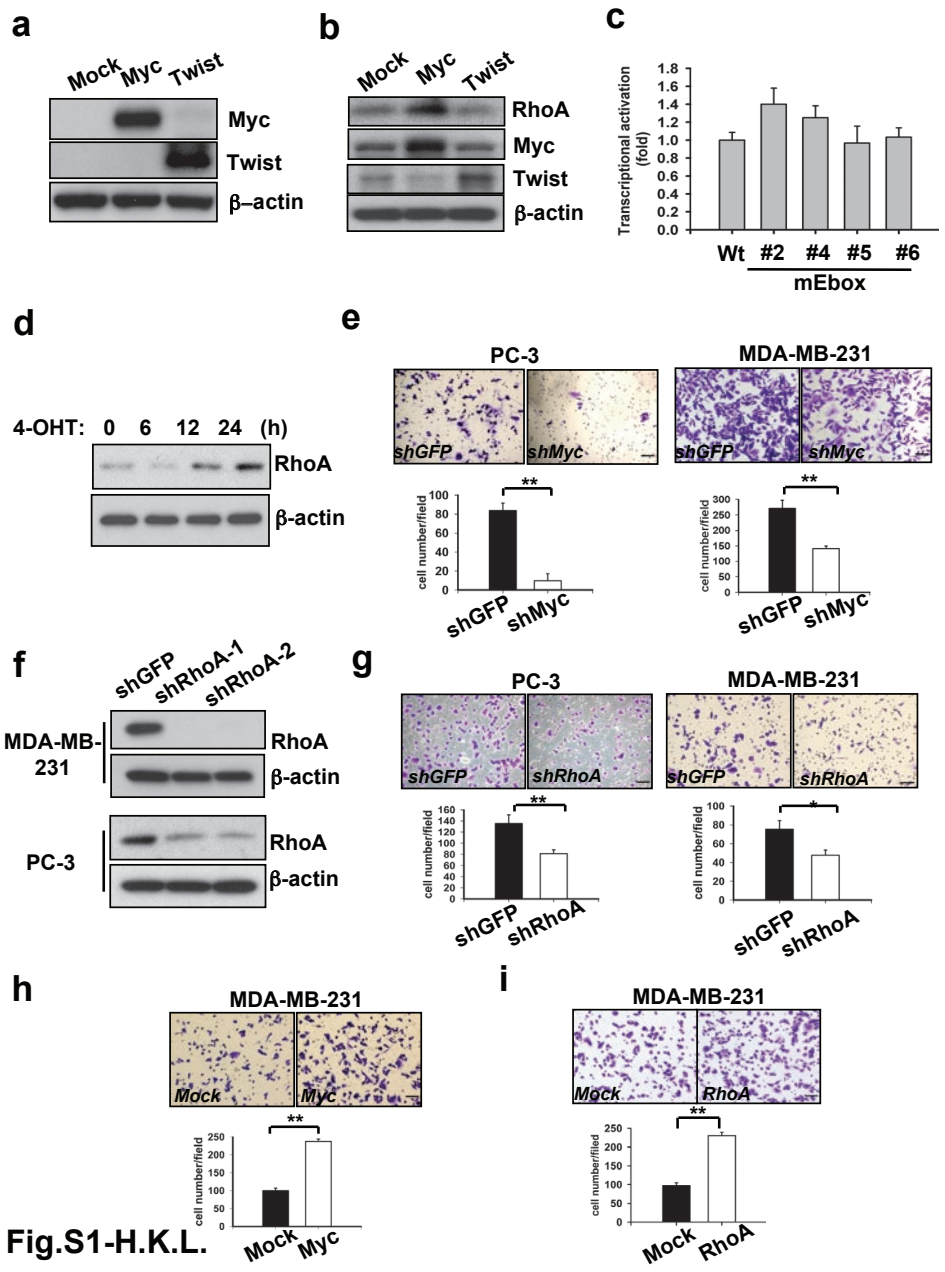

Fig.S1-H.K.L.

Figure S1 Myc regulates RhoA transcription and cell migration. **(a)** Western blot analysis showing the expression of constructs used in reporter assay in Fig. 1A as indicated. **(b)** Western blot analysis of RhoA expression in PC-3 cells transfected with the indicated plasmids. **(c)** Reporter assay in 293T cells transfected with various RhoA promoter constructs with mutations in different E-box regions. The results were shown as mean ± s.d. of one representative experiment (from 3 independent experiments) performed in triplicate. **(d)** Analysis of RhoA protein levels in MDA-MB-231 cell lines by western blot following the time course of MycER activation induced by 4-OHT. **(e)** Transwell cell migration assay in two cancer cell lines with GFP or Myc knockdown. **(f)** Western blot analysis of RhoA expression in two cancer lines with GFP or RhoA knockdown. Two RhoA lentiviral shRNAs were used in this assay. **(g)** Transwell cell migration assay in two cancer cell lines with GFP or RhoA knockdown. **(h)** Transwell cell migration assay in MDA-MB-231 cells infected with MSCV or MSCV-Myc. **(i)** Transwell cell migration assay in MDA-MB-231 cells infected with pcDNA3 or pcDNA3-RhoA. Results in panel **e, g, h, i** were shown as mean ± s.d. (n=4). Scale bar = 100 μm.

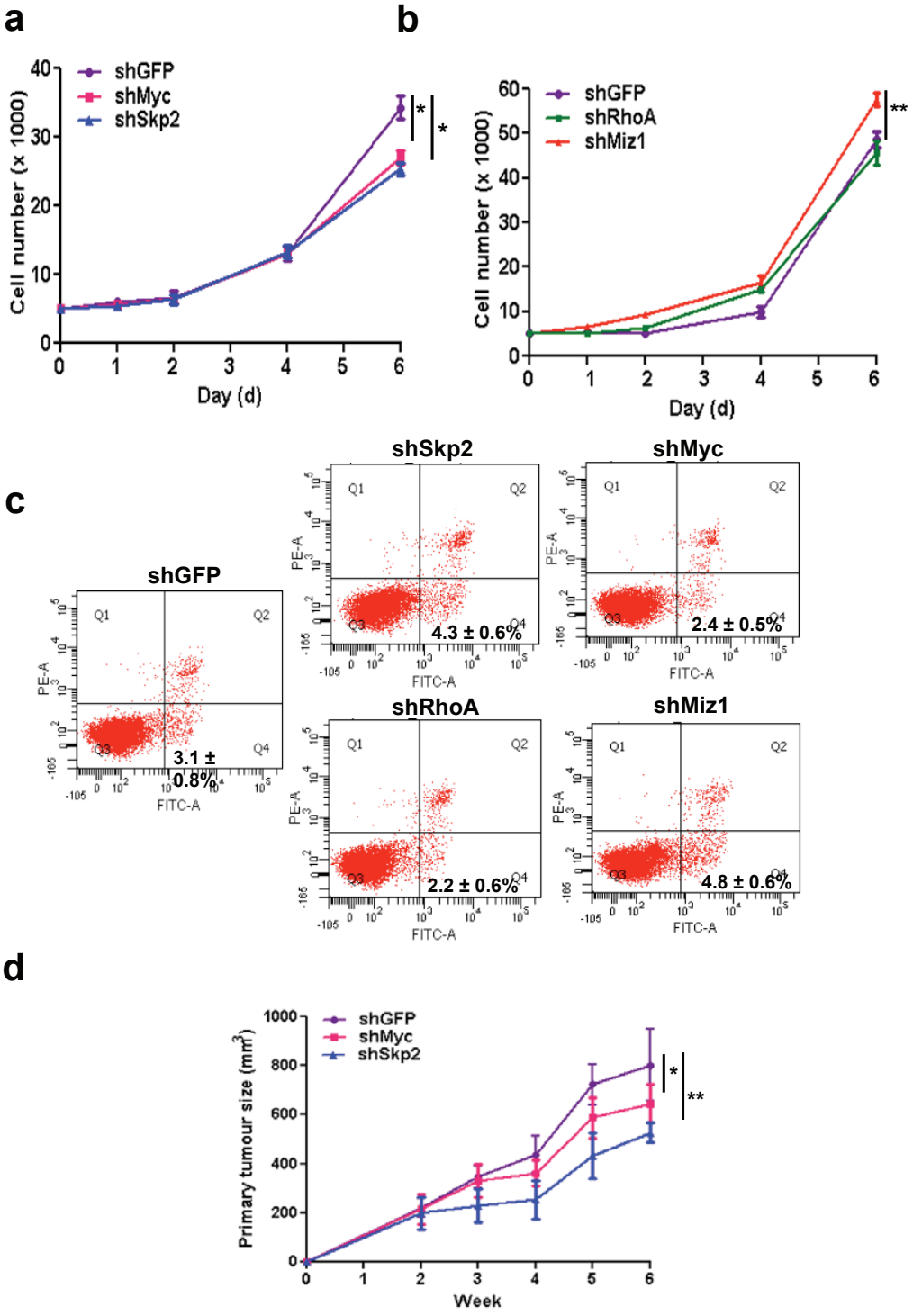

Figure S2 The effects of Myc, Skp2, Miz1, or RhoA silencing on cell growth and apoptosis. **(a, b)** *In vitro* cell growth assay in MDA-MB-231 cells silenced with GFP, Myc, Skp2, Miz1, or RhoA. **(c)** Cell apoptosis assay in MDA-MB-231 cells silenced with GFP, Myc, Skp2, Miz1, or RhoA. **(d)** The effect of Skp2 and Myc on primary tumour formation. MDA-MB-231 cells silenced with GFP, Myc, or Skp2 were injected into node mice nude mice. Results in panel **a-d** were presented as mean ± s.d. (panel a-c, n=3; panel d, n=6 for each group). * indicates $p<0.05$; ** indicates $p<0.01$.

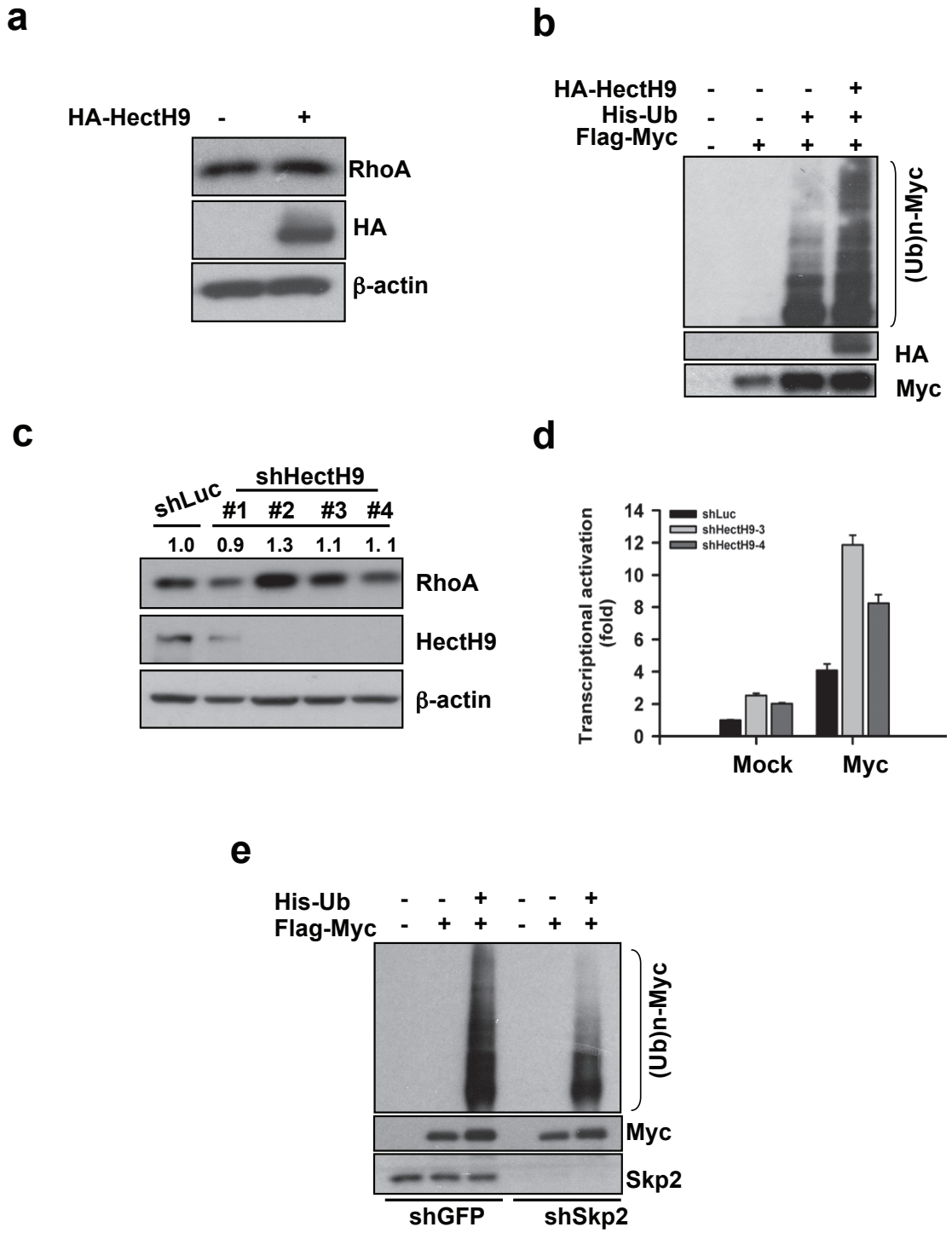

Figure S3 HectH9 is not required for RhoA gene and protein expression. **(a)** *In vivo* ubiquitination assay in 293T cells transfected with the indicated plasmids. **(b)** Western blot analysis of RhoA expression in 293T cells transfected with the indicated plasmids. **(c)** Western blot analysis of HectH9 and RhoA expression in 293T cells with Luciferase or HectH9 knockdown. Four HectH9 lentiviral shRNAs were used in this assay. **(d)** RhoA reporter assay in 293T cells with Luciferase or HectH9 knockdown. Two HectH9 lentiviral shRNAs were used in this assay. The results were shown as mean ± s.d. of one representative experiment (from 3 independent experiments) performed in triplicate. **(e)** *In vivo* ubiquitination assay in GFP- or Skp2-silenced 293T cells transfected with the indicated plasmids.

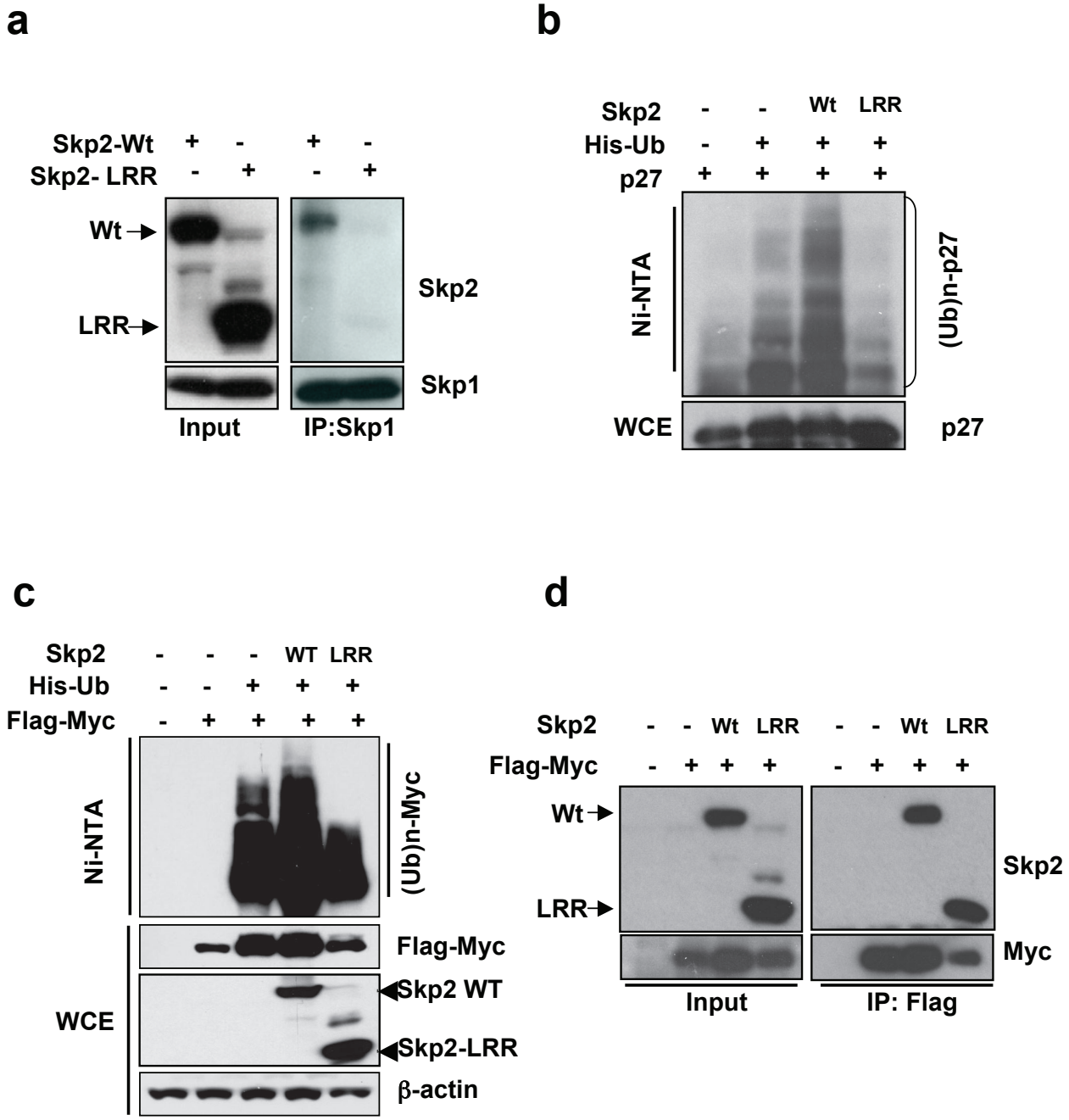

Figure S4 Skp2-LRR mutant loses its E3 ligase activity. **(a)** Co-immunoprecipitation assay in 293T cells transfected with the indicated plasmids. **(b, c)** *In vivo* ubiquitination assay in 293T cells transfected with the indicated plasmids. **(d)** Co-immunoprecipitation assay in 293T cells transfected with Wt Skp2 or Skp2-LRR.

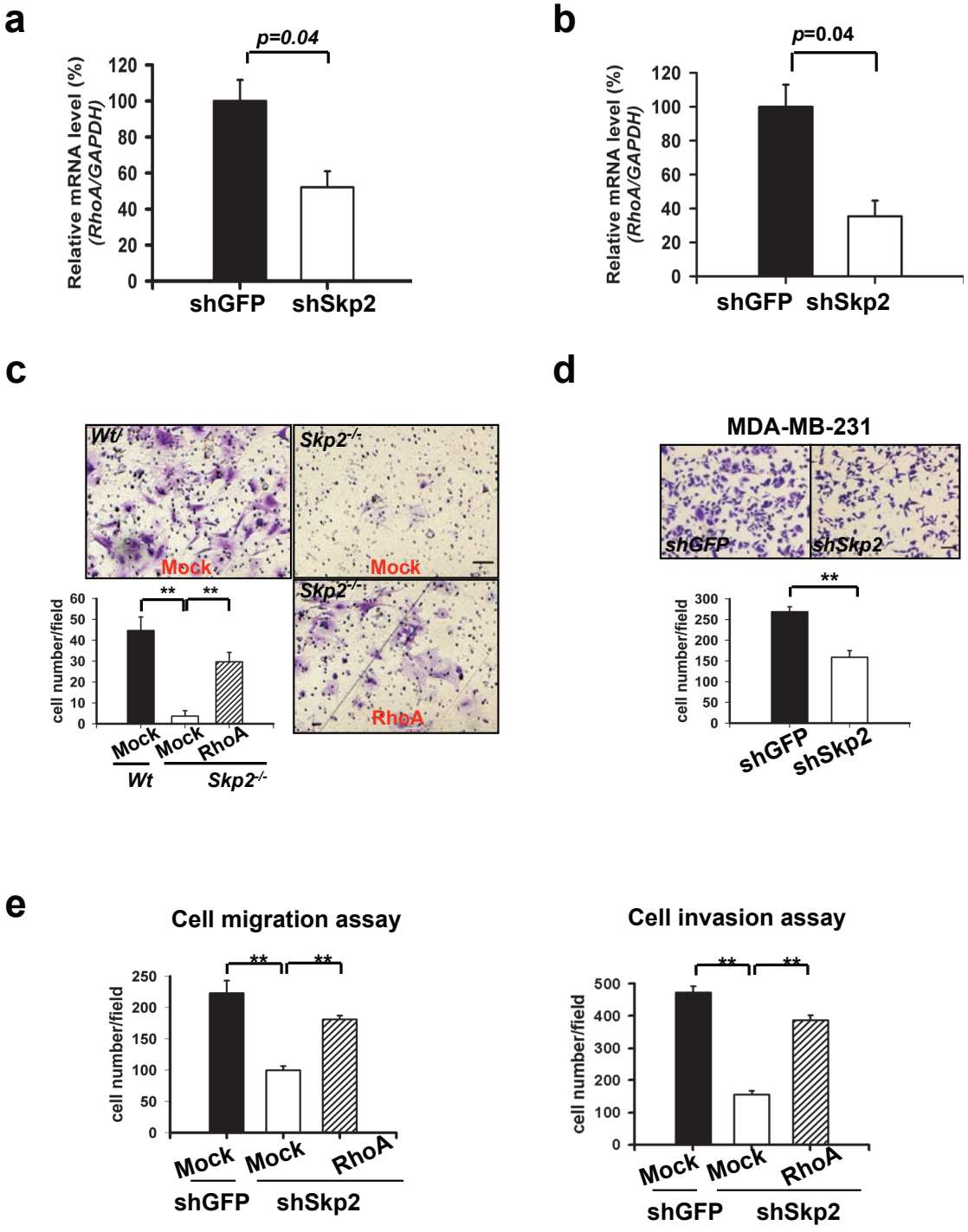

Figure S5 Skp2 regulates RhoA mRNA level and RhoA-dependent cell migration and invasion. **(a, b)** Real-time PCR analysis was performed in PC3 and MDA-MB-231 cells. **(c)** Transwell cell migration assay and Western blot analysis of RhoA expression in *Wt* and *Skp2*$^{-/-}$ primary MEFs infected with MSCV or MSCV-RhoA. **(d)** Transwell cell migration assay in MDA-MB-231cells with GFP or Skp2 knockdown. **(e)** Transwell cell migration assay and Matrigel cell invasion assay in MDA-MB-231 cells with GFP, Skp2 knockdown, or Skp2 knockdown plus RhoA overexpression. Results in panel **a-e** were presented as mean ± s.d. (panel a-b, n=3; panel c-e, n=4). Scale bar = 100 μm.

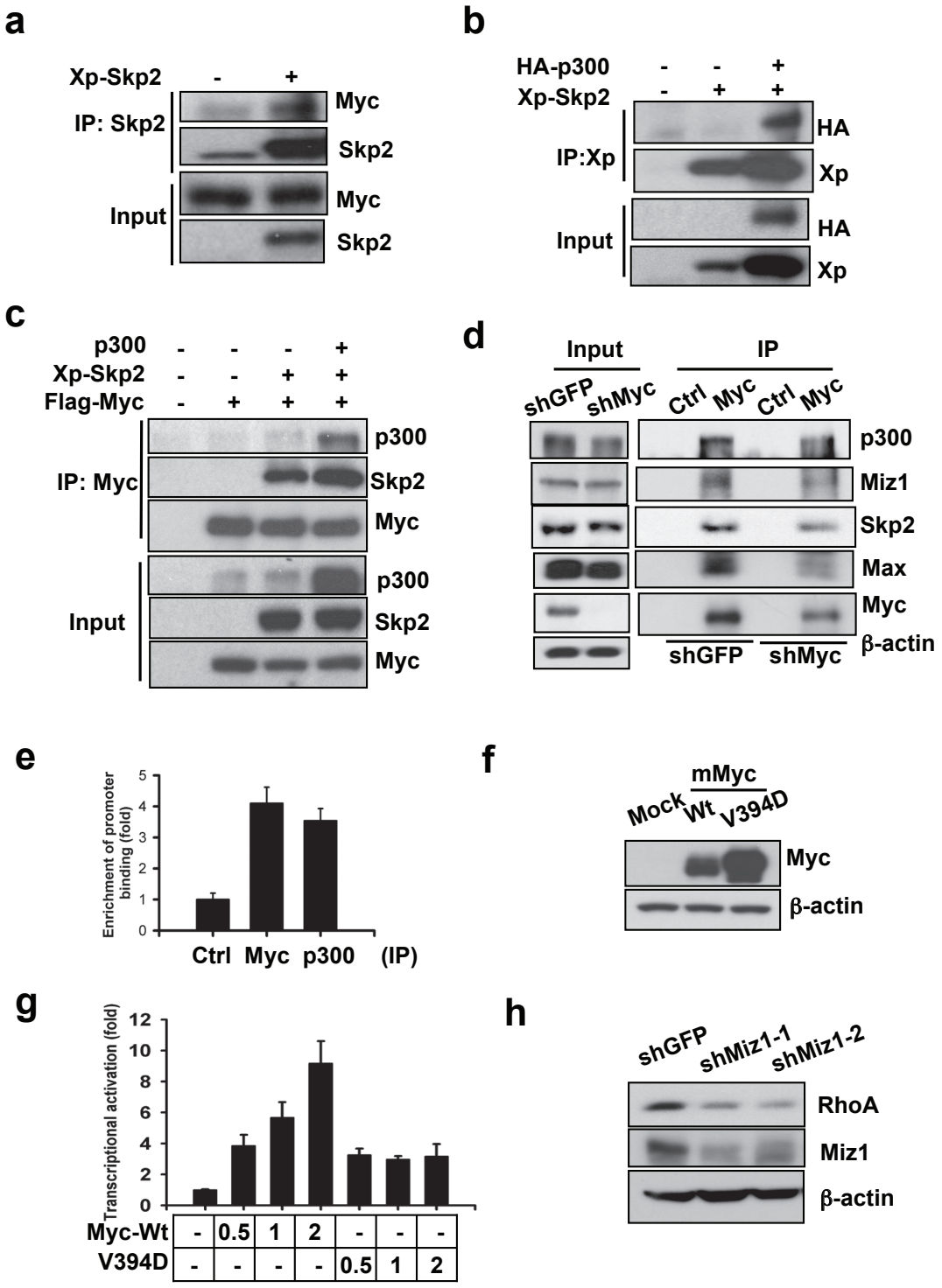

Figure S6 The RhoA transcription complex consists of Myc, Max, Skp2, Miz1, and p300. **(a-c)** The Myc immunocomplex consists of Myc, Max, Skp2, Miz1, and p300. Co-immunoprecipitation assay in 293T cells transfected with the indicated plasmids. **(d)** Co-immunoprecipitation assay in 293T cells with GFP and Myc knockdown. Total cell lysates were immunoprecipitated with Myc antibody, followed by Western blot analysis. **(e)** ChIP assay followed by real-time PCR analysis using various antibodies for immunoprecipitation as indicated in PC-3 cells. The quantified results were presented as mean ± s.d. (n=3). **(f, g)** The effect of MycV394D mutant on RhoA transcription. Western blot analysis in 293T cells transfected with mouse Wt Myc and mouse MycV394D mutant. Reporter assay in 293T cells transfected with Wt Myc and MycV394D mutant in a dose-dependent manner. The results were shown as mean ± s.d. of one representative experiment (from 3 independent experiments) performed in triplicate. **(h)** The effect of Miz1 on RhoA protein expression. Western blot analysis in MDA-MB-231 cells with GFP or Miz1 knockdown. Two Miz1 lentiviral shRNAs were used in this assay.

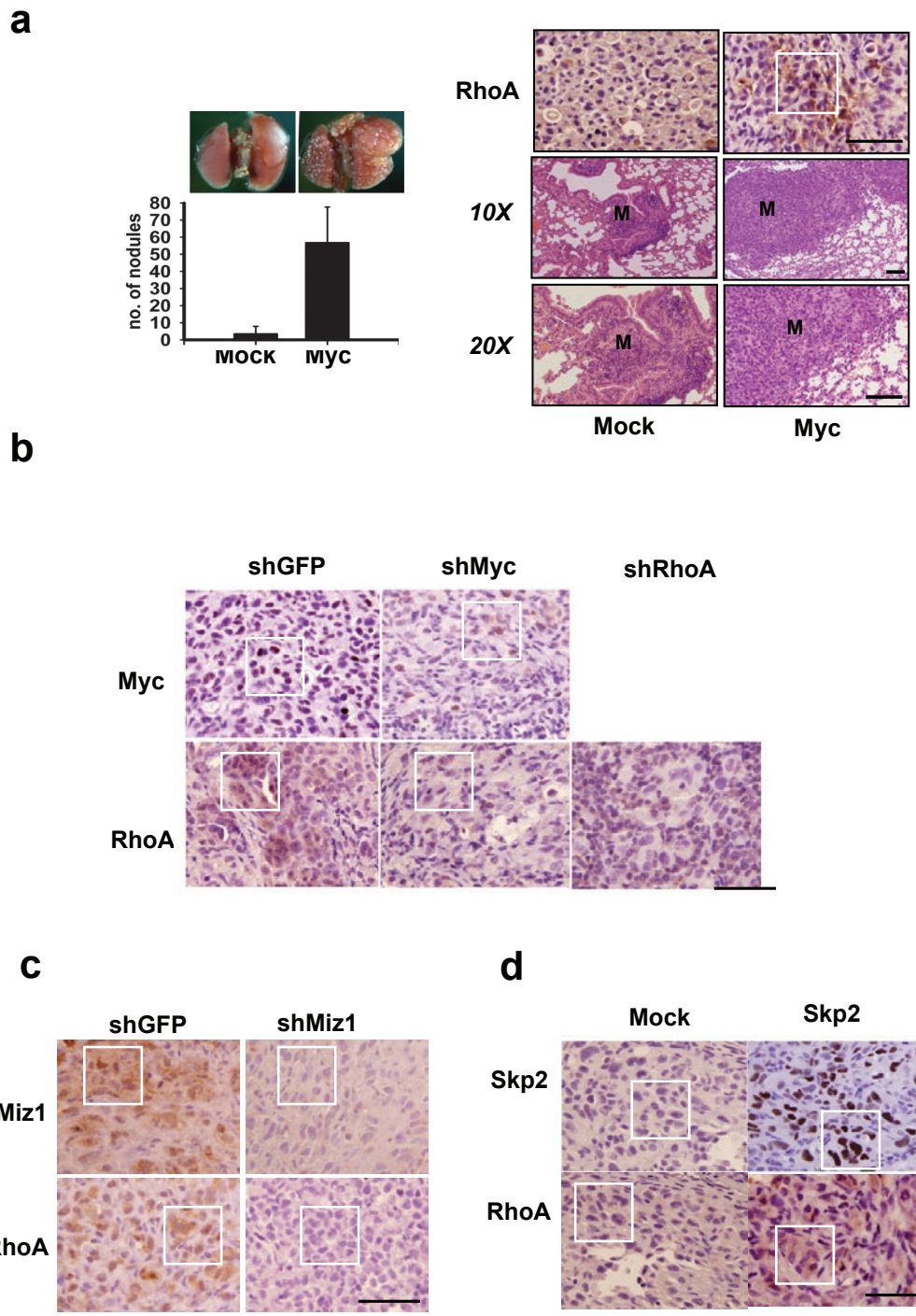

Figure S7 The Myc/Skp2/Miz1 complex regulates RhoA expression in metastatic breast tumours in the lung. **(a)** Lung metastasis assay and histological analysis from nude mice injected with MDA-MB-231 cells infected with MSCV or MSCV-Myc. Immunohistochemistry (IHC) of RhoA protein expression in metastatic breast tumour in the lung obtained from nude mice injected with MDA-MB-231 cells with MSCV or MSCV-Myc. The quantified results were presented as mean ± s.d. (n = 6 for each group) **(b)** Immunohistochemistry (IHC) of Myc and RhoA protein expression in metastatic breast tumour in the lung obtained from nude mice injected with MDA-MB-231 cells with GFP, Myc, or RhoA knockdown. **(c)** IHC of Miz1 and RhoA protein expression in metastatic breast tumour in the lung obtained from nude mice injected with MDA-MB-231 cells with GFP or Miz1 knockdown. **(d)** IHC of Skp2 and RhoA protein expression in metastatic breast tumour in the lung obtained from nude mice injected with MDA-MB-231 cells infected with pBabe, and pBabe-Skp2-Wt. The white box was highlighted to show distinct protein expression for Myc, Skp2, Miz1, and RhoA. The results in Supplementary information Fig. S7 showed that Miz1, Myc, and RhoA knockdown in MDA-MB-231 dramatically reduced the IHC signal for Miz1, Myc, and RhoA compared with GFP knockdown control, respectively, suggesting that these antibodies used in our IHC study are very specific. Scale bar = 100 μm.

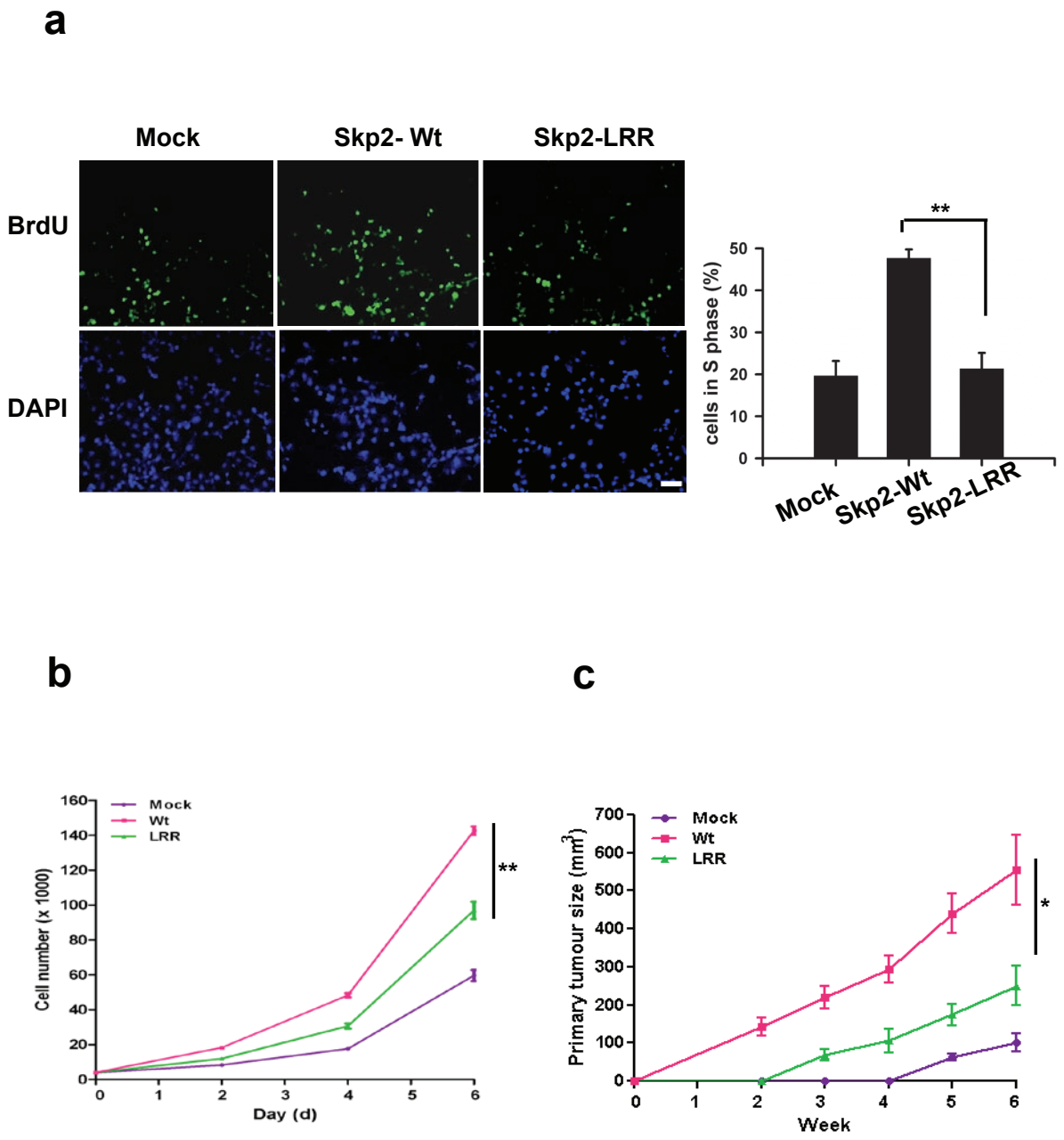

Figure S8 SCF-Skp2 E3 ligase activity is required for Skp2-mediated cell cycle entry, cell proliferation, and primary tumour formation. **(a)** The BrdU incorporation assay in COS-1 cells transfected with mock, Wt Skp2, or Skp2-LRR. The representative image as indicated were shown in left panel; the quantified results were shown in right panel. The results were presented as mean ± s.d. (n=3). Green: BrdU-FLUOS; Blue: DAPI. **(b)** *In vitro* cell growth assay in MDA-MB-231 cells infected with mock, Wt Skp2, or Skp2-LRR. **(c)** *In vivo* primary tumour growth in MDA-MB-231 cells infected with mock, Wt Skp2, or Skp2-LRR. Cells were injected into nude mice, and tumourigenesis was monitored. The results are presented as mean ± s.d. (n = 6 for each group). * indicates $p<0.05$; ** indicates $p<0.01$. Scale bar = 20 μm.

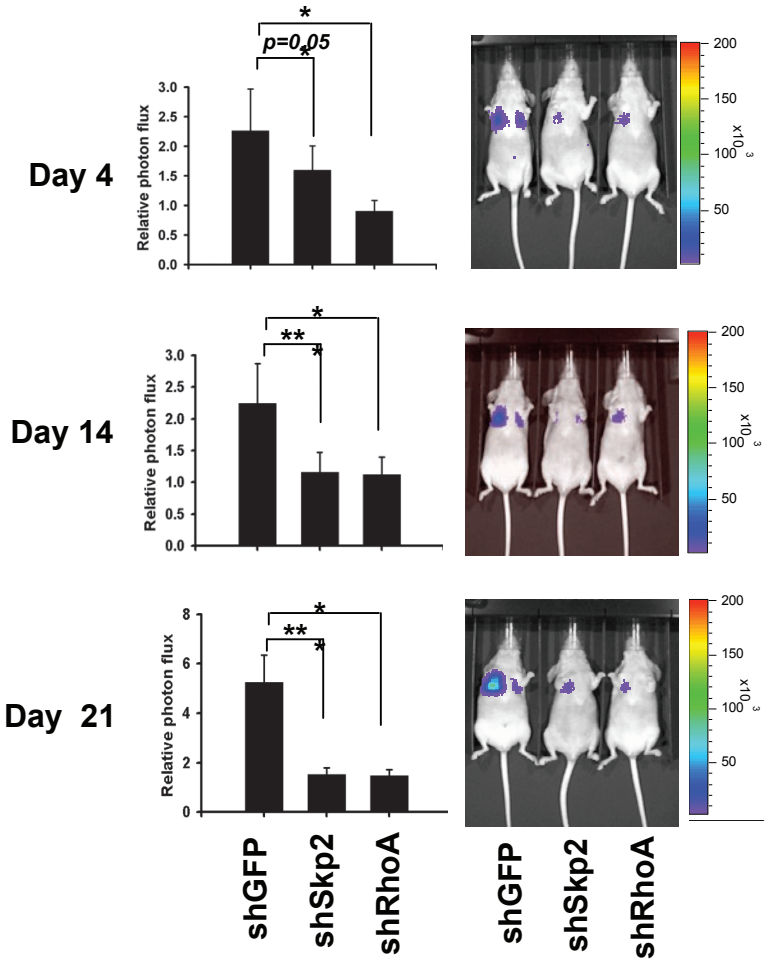

Figure S9 Skp2 and RhoA regulate lung colonization of breast cancer cells and subsequent metastasis. MDA-MB-231-Luc cells with GFP, Skp2, or RhoA knockdown were injected to the nude mice, and the kinetics of breast cancer metastasis to the lung were measured by bioluminescence and quantified. Representative bioluminescent images were shown in day 4, 14, and 21. The results are presented as mean ± s.d. (n = 7 for each group). * indicates $p<0.05$; ** indicates $p<0.01$.

a

Parameters	Status at presentation	
	Localized	Metastatic
RhoA LI	35.74 ± 27.690	55.14 ± 34.003
Myc LI	16.85 ± 22.453	30.62 ± 28.365
Skp2 LI	2.67 ± 3.700	7.19 ± 6.666
Miz-1 LI	20.19 ± 25.664	37.97 ± 30.401

b

Correlation	Myc	Skp2	Miz-1
RhoA	r=0.282	r=0.333	R=0.462
	p=0.024*	**p=0.007****	**p<0.001****
Myc		r=0.398	r=0.426
		p=0.001**	**p<0.001****
Skp2			r=0.432
			P<0.001**

Figure S10 The Myc/Skp2 complex is correlated with RhoA expression in metastatic prostate cancer. (**a**) Expression level of RhoA, Myc, and Skp2 in primary prostate cancer versus metastatic prostate cancer. (b) The correlations among the four markers were calculated by using Pearson's correlation test, and the differences in the labeling indices of the markers tested between cases with and without metastatic disease were compared by Student's t-test. * indicates $p<0.05$; ** indicates $p<0.01$.

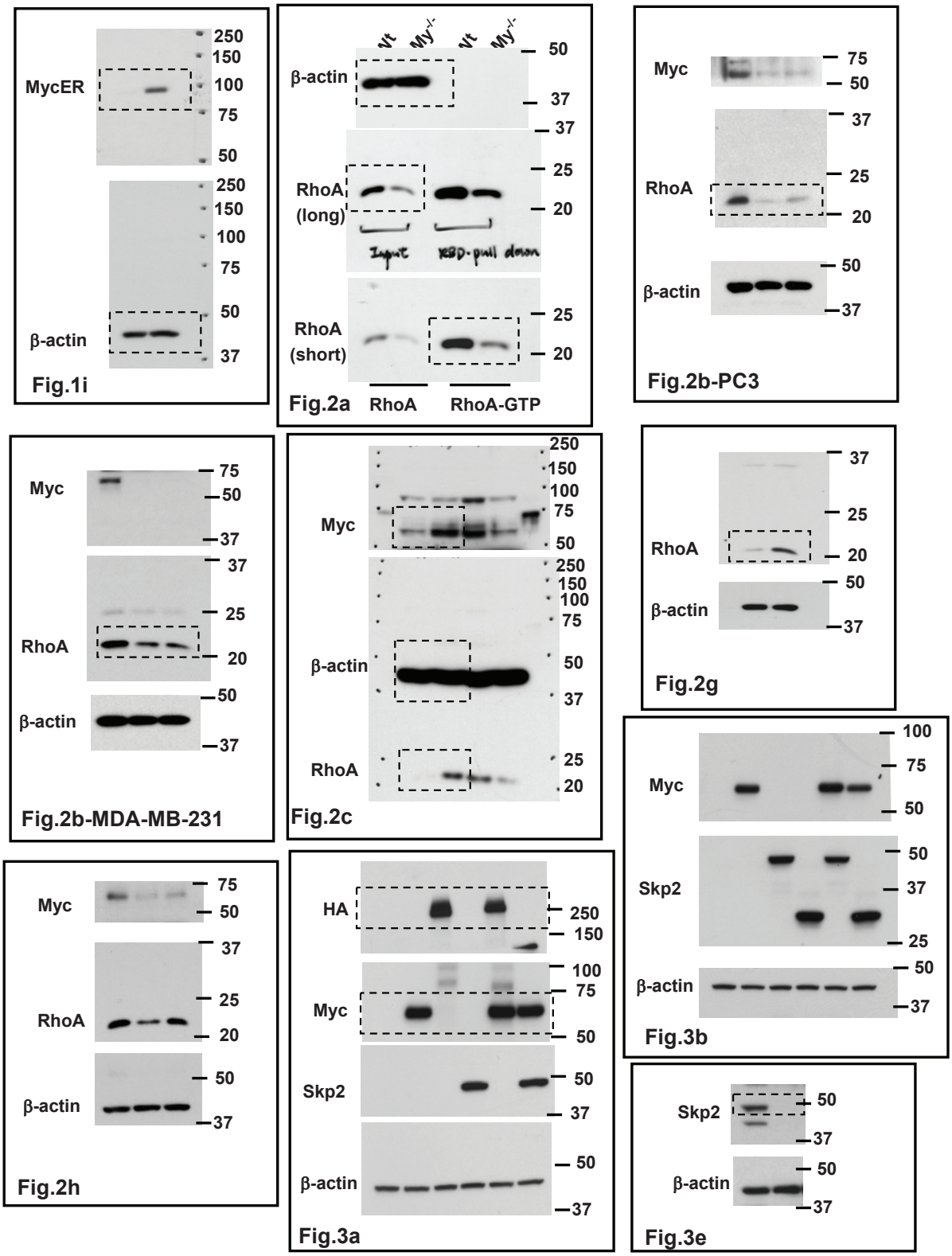

Figure S11 Full scans of western blots

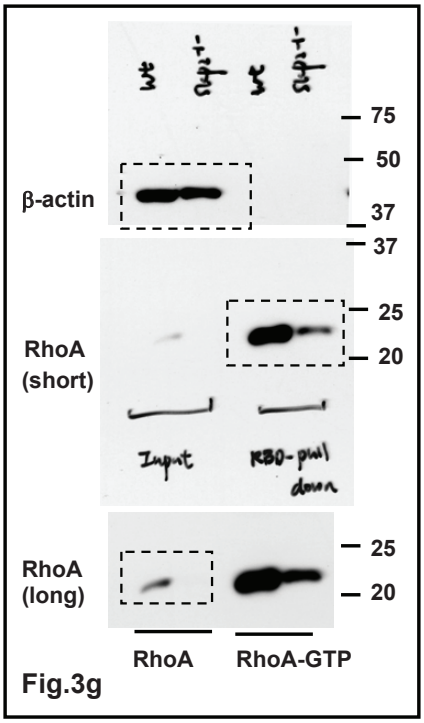

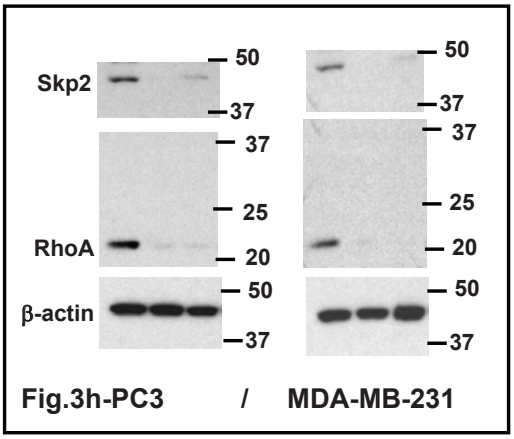

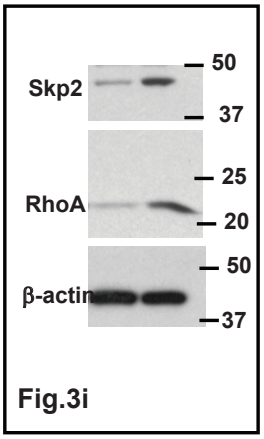

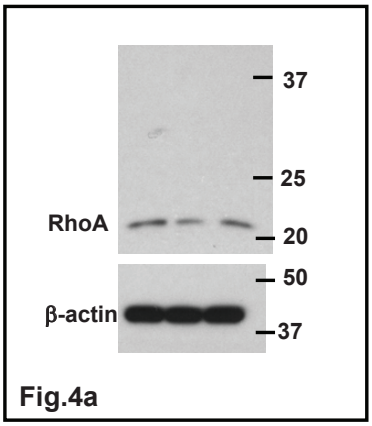

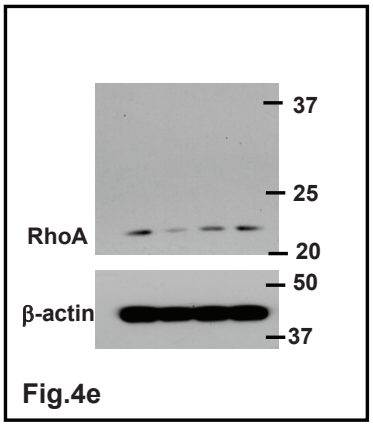

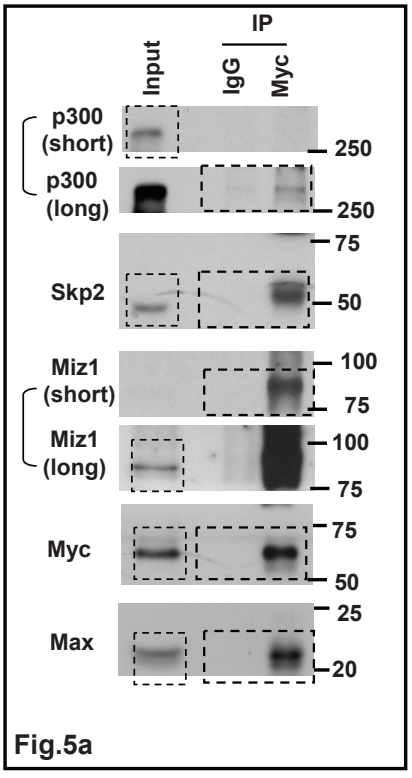

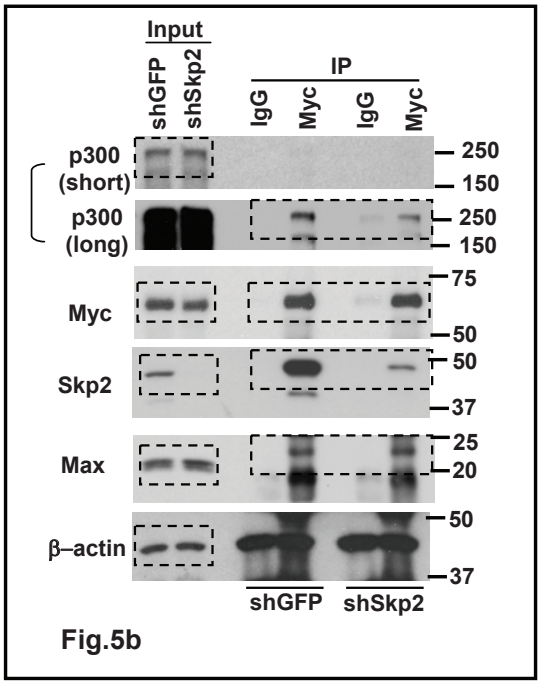

Figure S11 continued

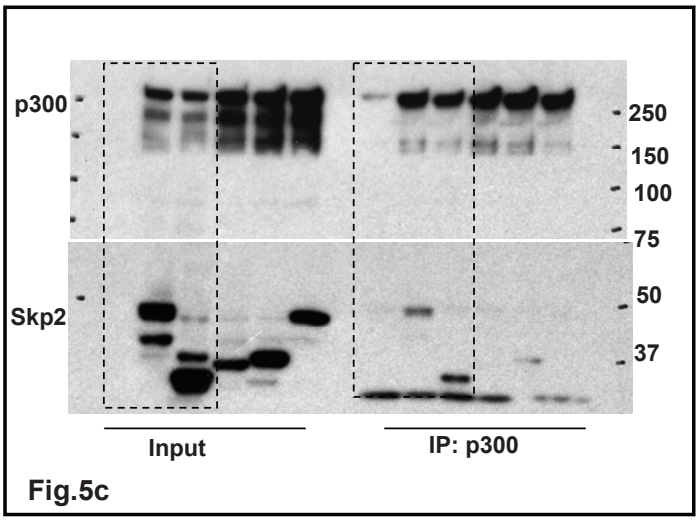

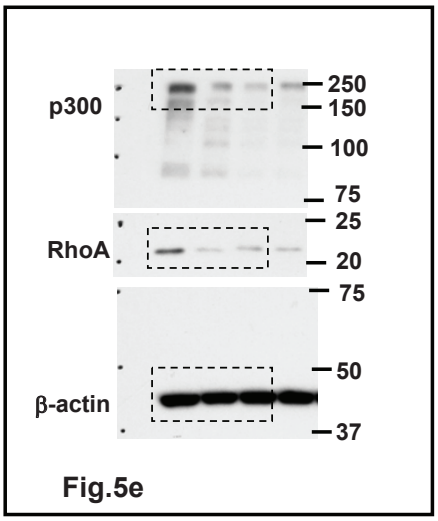

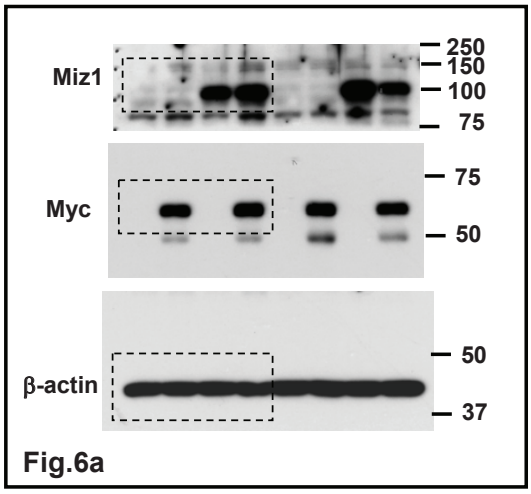

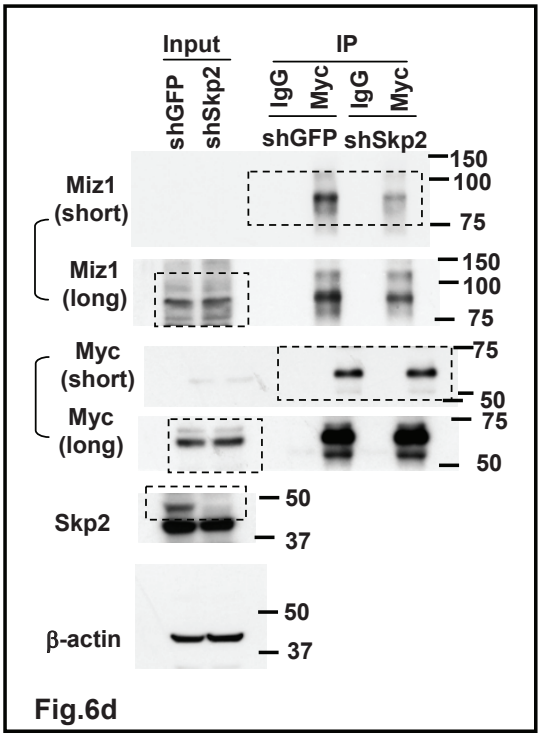

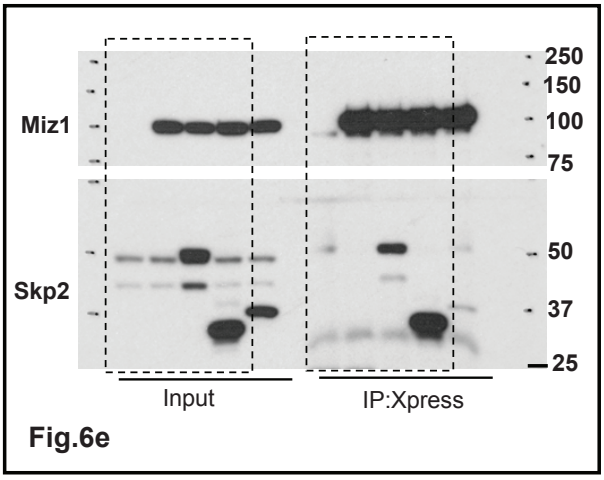

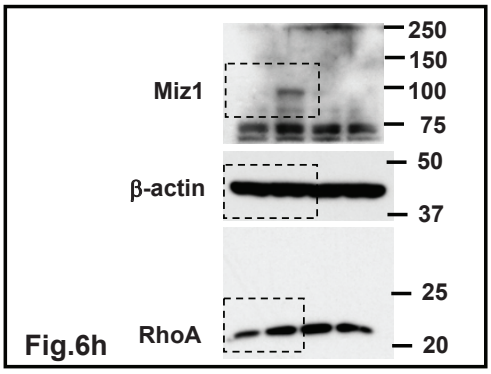

Figure S11 continued